Space–time adaptive splitting scheme for the numerical simulation of polycrystallization

Ronald H. W. Hoppe, B. Pahari, J. J. Winkle

Angaben zur Veröffentlichung / Publication details:

Hoppe, Ronald H. W., B. Pahari, and J. J. Winkle. 2022. "Space–time adaptive splitting scheme for the numerical simulation of polycrystallization." *Journal of Computational and Applied Mathematics* 404: 113882. https://doi.org/10.1016/j.cam.2021.113882.

Space–time adaptive splitting scheme for the numerical simulation of polycrystallization

R.H.W. Hoppe [a,b,*,1], B. Pahari [c], J.J. Winkle [d]

[a] *Department of Mathematics, University of Augsburg, Germany*
[b] *Department of Mathematics, University of Houston, USA*
[c] *Aero-Propulsion, Mechatronics, and Energy Center, Florida State University, USA*
[d] *Department of BioSciences, Rice University, USA*

1. Introduction

Polycrystallization of thin films is a dynamic process that can be described by a phase field model featuring a free energy in two or three phase field variables, namely the local degree of crystallinity, the orientation angle, and the local concentration. The model includes isotropic and anisotropic growth of the crystals and the structure of the orientational free energy may allow for crystalline branching in the form of spherulites due to misorientations at low grain boundaries. Due to their low surface roughness at the nanoscale and their thermodynamic stability, polycrystalline thin films are of particular interest for diffraction gratings, photonic band gap structures, and coatings based on structural colors instead of pigments. We refer to the survey articles [1,2] and the references therein.

From a mathematical point of view, the orientational free energy is related to the total variation of the orientation angle and thus has to be considered in the Banach space of functions of bounded variation as has been done in [3,4] for a two-field and in [5] for a three-field phase field model for polycrystalline growth in binary mixtures. The numerical solution of

* Corresponding author at: Department of Mathematics, University of Houston, USA.
E-mail addresses: hoppe@math.uni-augsburg.de, rohop@math.uh.edu (R.H.W. Hoppe), bpahari@fsu.edu (B. Pahari), winkle@rice.edu (J.J. Winkle).

[1] The work of the authors has been supported by the NSF, USA grant DMS-1520886.

the phase field models in [3–5] was based on a splitting scheme featuring an implicit discretization in time with adaptive time stepping and a discretization in space by standard finite elements with respect to a shape-regular triangulation of the computational domain. However, adaptivity in space has not been considered despite the fact that the solution exhibits very narrow interior transition regions with extremely steep slopes. Therefore, this contribution is devoted to a space–time adaptive splitting method where the adaptivity in space is taken care of by equilibrated a posteriori error estimators. As far as the theory of equilibrated a posteriori error estimators is concerned, we refer to [6–11].

The paper is organized as follows: In Section 2, we provide basic notations and results with emphasis on the Banach space BV of functions of bounded variation. Section 3 is devoted to the phase field model in the local degree of crystallinity ϕ and the orientation angle Θ as phase field variables. In particular, we consider both an orientational free energy density as in the classical Kobayashi–Warren–Carter model [12] (cf. also [3,5]) and an orientational free energy density with a misorientation of the orientation angle as has been dealt with in [4]. In the following Section 4 we suggest a splitting scheme based on an implicit discretization in time which decouples the evolutionary problems such that at each time step minimization problems for ϕ in the Sobolev space $W^{1,2}$ and for Θ in the space BV of functions of bounded variation have to be solved successively. Both problems admit a solution as can be shown by tools from the calculus of variations. Section 5 deals with a further discretization in space by standard finite elements for the problem in ϕ and by an IPDG approximation for the problem in Θ. Section 6 addresses the construction of equilibrated a posteriori error estimators for the spatial discretization errors in ϕ and Θ which amounts to the proper specification of flux functions in the space $\underline{\mathbf{H}}(\mathrm{div};\Omega)$. In Section 7, the nonlinear algebraic system in Θ, resulting from the IPDG approximation, is numerically solved by a predictor–corrector continuation strategy featuring constant continuation as a predictor and a semismooth Newton method as a corrector allowing for an adaptive choice of the time steps. Finally, in Section 8 we provide a documentation of numerical results for two illustrative polycrystallization processes.

2. Notations and basic results

For an open or closed set $A \subset \mathbb{R}^d, d \in \mathbb{N}$, we denote by $C_0^m(A;\mathbb{R}^d), 0 \le m < \infty$, the Banach space of m-times continuously differentiable vector-valued functions $\mathbf{q} = (q_1, \dots, q_d)$ with compact support in A. In case $m = 0$ we write $C_0(A;\mathbb{R}^d)$ instead of $C_0^0(A;\mathbb{R}^d)$ and in case $d = 1$ we write $C_0^m(A)$ instead of $C_0^m(A;\mathbb{R}^1)$. We further refer to $C_0^\infty(A)$ as the linear space of infinitely smooth (scalar) functions with compact support in A and to $\mathcal{D}(A)$ as its dual space of distributional derivatives.

By $\mathcal{M}(A;\mathbb{R}^d), d \in \mathbb{N}$, we denote the Banach space of vector-valued bounded Radon measures $\boldsymbol{\mu} = (\mu_1, \dots, \mu_d)$ equipped with the total variation norm

$$|\boldsymbol{\mu}|(A) := \sup\{\sum_{n=1}^{\infty} |\boldsymbol{\mu}(A_n)| \mid A = \bigcup_{n=1}^{\infty} A_n, A_n \cap A_m = \emptyset \text{ for } n \neq m\}, \tag{2.1}$$

where $\{A_n\}_{\mathbb{N}}$ is a sequence of mutually disjoint subsets of A such that $A = \bigcup_{n=1}^{\infty} A_n$, and we refer to $\mathcal{M}^+(A;\mathbb{R}^d)$ as the set of positive Radon measures.

In view of the Riesz representation theorem $\mathcal{M}(A;\mathbb{R}^d)$ is the dual space of $C_0(A;\mathbb{R}^d)$ with the duality pairing

$$\langle \boldsymbol{\mu}, \mathbf{q}\rangle_{\mathcal{M},C_0} := \int_\Omega \mathbf{q}\, d\boldsymbol{\mu} = \sum_{i=1}^{d} \int_A q_i\, d\mu_i. \tag{2.2}$$

A sequence $\{\boldsymbol{\mu}_n\}_{\mathbb{N}}$ of Radon measures $\boldsymbol{\mu}_n \in \mathcal{M}(A;\mathbb{R}^d), n \in \mathbb{N}$, is said to converge weakly* to $\boldsymbol{\mu} \in \mathcal{M}(A;\mathbb{R}^d)$ ($\boldsymbol{\mu}_n \rightharpoonup^* \boldsymbol{\mu}$ ($n \to \infty$)) if

$$\langle \boldsymbol{\mu}_n, \mathbf{q}\rangle_{\mathcal{M},C_0} \to \langle \boldsymbol{\mu}, \mathbf{q}\rangle_{\mathcal{M},C_0} \ (n \to \infty) \quad \text{for all } \mathbf{q} \in C_0^\infty(A;\mathbb{R}^d). \tag{2.3}$$

For a bounded Lipschitz domain $\Omega \subset \mathbb{R}^d, d \in \mathbb{N}$, with boundary $\Gamma = \partial\Omega$ we refer to $L^p(\Omega;\mathbb{R}^d), 1 \le p < \infty$, as the Banach space of pth power Lebesgue integrable vector-valued functions on Ω with norm $\|\cdot\|_{L^p(\Omega;\mathbb{R}^d)}$ and to $L^\infty(\Omega;\mathbb{R}^d)$ as the Banach space of essentially bounded vector-valued functions on Ω with norm $\|\cdot\|_{L^\infty(\Omega;\mathbb{R}^d)}$. In case $d = 1$ we will write $L^p(\Omega)$ instead of $L^p(\Omega;\mathbb{R}^1)$. Further, we denote by $W^{1,p}(\Omega), 1 \le p \le \infty$, the Sobolev spaces with norms $\|\cdot\|_{W^{1,p}(\Omega)}$ and by $W_0^{1,p}(\Omega), 1 < p < \infty$, the closure of $C_0^\infty(\Omega)$ with respect to the $\|\cdot\|_{W^{1,p}}$ norm. We note that for $1 < p < \infty$ the Sobolev space $W^{1,p}(\Omega)$ is reflexive with dual space $W^{1,q}(\Omega)$, $1/p + 1/q = 1$. For $p = 1$ the dual space of the Sobolev space $W^{1,1}(\Omega)$ is $W^{1,\infty}(\Omega)$. However, the Sobolev space $W^{1,1}(\Omega)$ is not reflexive. We further note that for $p = 2$ the spaces $L^2(\Omega;\mathbb{R}^d)$ and $W^{1,2}(\Omega) = H^1(\Omega)$ are Hilbert spaces with inner products $(\cdot,\cdot)_{L^2(\Omega;\mathbb{R}^d)}$ and $(\cdot,\cdot)_{W^{1,2}(\Omega)}$.

A sequence $\{u_n\}_{\mathbb{N}}$ of functions $u_n \in W^{1,p}(\Omega), n \in \mathbb{N}, 1 < p < \infty$, is said to converge weakly to $u \in W^{1,p}(\Omega)$ ($u_n \rightharpoonup u$ ($n \to \infty$)), if it holds

$$\langle v, u_n\rangle_{W^{1,q},W^{1,p}} \to \langle v, u\rangle_{W^{1,q},W^{1,p}} \ (n \to \infty) \quad \text{for all } v \in W^{1,q}(\Omega),\ 1/p + 1/q = 1.$$

Lemma 2.1. *Let $\{u_n\}_{\mathbb{N}}$ be a bounded sequence of functions $u_n \in W^{1,p}(\Omega), n \in \mathbb{N}, 1 < p < \infty$. Then there exist a subsequence $\mathbb{N}' \subset \mathbb{N}$ and a function $u \in W^{1,p}(\Omega)$ such that*

$$u_n \rightharpoonup u \ (\mathbb{N}' \ni n \to \infty) \quad \text{in } W^{1,p}(\Omega). \tag{2.4}$$

Proof. We refer to [13].

A functional $F : W^{1,p}(\Omega) \to \mathbb{R}$, $1 < p < \infty$, is said to be weakly sequential lower semicontinuous in $W^{1,p}(\Omega)$ if for every sequence $\{u_n\}_{\mathbb{N}}$ of functions $u_n \in W^{1,p}(\Omega)$, $n \in \mathbb{N}$, such that $u_n \rightharpoonup u$ $(n \to \infty)$ in $W^{1,p}(\Omega)$ for some $u \in W^{1,p}(\Omega)$ it holds

$$F(u) \le \liminf_{n\to\infty} F(u_n). \tag{2.5}$$

A function $u \in L^1(\Omega)$ is said to be of bounded variation if its distributional derivative Du satisfies $Du \in \mathcal{M}(\Omega; \mathbb{R}^d)$, i.e., for all $\mathbf{q} \in C_0^1(\Omega; \mathbb{R}^d)$ we have

$$-\int_\Omega \nabla \cdot \mathbf{q} u \, dx = \int_\Omega \mathbf{q} \cdot dDu.$$

The total variation of u is defined as follows

$$|Du|(\Omega) := \sup \{-\int_\Omega \nabla \cdot \mathbf{q}\, u \, dx \mid \mathbf{q} \in C_0^1(\Omega; \mathbb{R}^d), |\mathbf{q}| \le 1 \text{ in } \Omega\}. \tag{2.6}$$

We denote by $BV(\Omega)$ the Banach space of functions $u \in L^1(\Omega)$ such that $|Du|(\Omega) < \infty$ equipped with the norm

$$\|u\|_{BV(\Omega)} := \|u\|_{L^1(\Omega)} + |Du|(\Omega). \tag{2.7}$$

Clearly, we have $W^{1,1}(\Omega) \subset BV(\Omega)$ and $u \in W^{1,1}(\Omega)$ iff $u \in L^1(\Omega)$ and Du is absolutely continuous with respect to the Lebesgue measure. In particular, we have the Lebesgue–Radon–Nikodym decomposition

$$Du = \nabla u + D^s u, \tag{2.8}$$

where $\nabla u \in L^1(\Omega; \mathbb{R}^d)$ is called the approximate gradient of u and $D^s u \in \mathcal{M}(\Omega; \mathbb{R}^d)$ is said to be the singular part of the derivative.

Functions $u \in BV(\Omega)$ have a trace $u|_\Gamma \in L^1(\Gamma)$. The trace mapping $T : BV(\Omega) \to L^1(\Gamma)$ is linear, continuous from $BV(\Omega)$ endowed with the strict topology to $L^1(\Gamma)$ equipped with the strong topology (cf., e.g., Theorem 10.2.2 in [14]). The subspace $BV_0(\Omega)$ of $BV(\Omega)$ is the kernel of the trace mapping T. It is a Banach space equipped with the induced norm. For $u_D \in L^1(\Gamma)$ we further set $BV_{u_D,\Gamma}(\Omega) := \{u \in BV(\Omega) \mid Tu = u_D\}$.

A sequence $\{u_n\}_{\mathbb{N}}$ of functions $u_n \in BV(\Omega)$, $n \in \mathbb{N}$, is said to converge weakly* to $u \in BV(\Omega)$ if $u_n \to u$ in $L^1(\Omega)$ and $Du_n \rightharpoonup^* Du$ in $\mathcal{M}(\Omega; \mathbb{R}^d)$ as $\mathbb{N} \ni n \to \infty$.

Lemma 2.2. *Let $\{u_n\}_{\mathbb{N}}$ be a uniformly bounded sequence of functions $u_n \in BV(\Omega)$, $n \in \mathbb{N}$, i.e.,*

$$\|u_n\|_{BV(\Omega)} \le C \quad , n \in \mathbb{N},$$

for some $C > 0$. Then there exist a subsequence $\mathbb{N}' \subset \mathbb{N}$ and $u \in BV(\Omega)$ such that

$$u_n \rightharpoonup^* u \quad \text{in } BV(\Omega) \text{ as } \mathbb{N}' \ni n \to \infty.$$

Proof. We refer to [15].

A functional $F : BV(\Omega) \to \mathbb{R}$ is said to be weakly* sequential lower semicontinuous in $BV(\Omega)$ if for every sequence $\{u_n\}_{\mathbb{N}}$ of functions $u_n \in BV(\Omega)$, $n \in \mathbb{N}$, such that $u_n \rightharpoonup^* u$ $(n \to \infty)$ in $BV(\Omega)$ for some $u \in BV(\Omega)$ it holds

$$F(u) \le \liminf_{n\to\infty} F(u_n). \tag{2.9}$$

3. The phase field model

As a mathematical model for crystal growth in polycrystalline binary mixtures we use a phase field model where the free energy depends on two phase field variables. These are a structural order parameter ϕ measuring the local degree of crystallinity (volume fraction of the crystalline phase) and an orientation field Θ which locally describes the crystallographic orientation. Such phase field models have been widely suggested in the literature (we refer to the survey articles [1,2] and the references therein). We consider polycrystallization with and without orientational mismatch. The presence of orientational mismatch gives rise to the formation of spherulites (cf., e.g., [4,16]).

For a bounded domain $\Omega \subset \mathbb{R}^2$ with boundary $\Gamma = \partial\Omega$ the free energy reads as follows:

$$F(\phi, \Theta) = \int_\Omega \frac{1}{2} s(\nabla\phi, \Theta)^2 \, |\nabla\phi|^2 + g(\phi) + \frac{H}{2\xi_0} f_{ori}(\omega(\phi), \nabla\Theta) \quad dx. \tag{3.1}$$

Here, the functions $s = s(\nabla\phi, \Theta)$, $g(\phi)$, and $f_{ori}(\omega(\phi), \nabla\Theta)$ refer to an anisotropy function, a double well potential, and an orientational free energy density. The function ω is a continuously differentiable interpolation function given by

$$\omega(\eta) = \begin{cases} \varepsilon_r \ , \ \eta \le 0 \\ \varepsilon_r + 2(2 - 3\varepsilon_r)\eta^2 - 4(1 - \varepsilon_r)\eta^3 + \eta^4 \ , \ 0 \le \eta \le 1 \\ 1 - \varepsilon_r \ , \ \eta \ge 1 \end{cases} \quad , \ \eta \in \mathbb{R}, \tag{3.2}$$

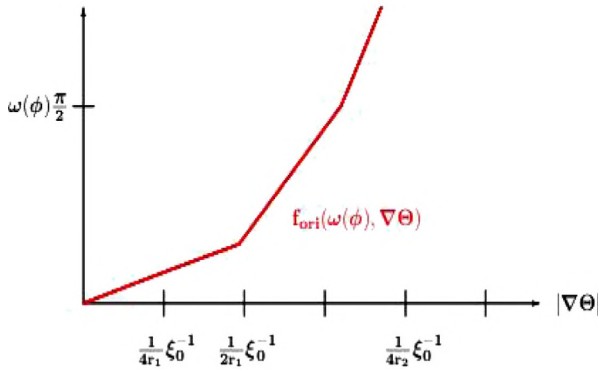

Fig. 1. The convexified orientational free energy density $f_{ori}(\omega(\phi), \nabla\Theta)$ in case of polycrystallization with orientational mismatch.

where $0 < \varepsilon_r \ll 1$. The function ω has the property

$$0 < \varepsilon_r \leq \omega(\eta) \leq 1 - \varepsilon_r, \quad \eta \in \mathbb{R}. \tag{3.3}$$

Moreover, the anisotropy function $s(\boldsymbol{\eta}, \gamma)$, $\boldsymbol{\eta} = (\eta_1, \eta_2)^T \in \mathbb{R}^2$, $\gamma \in \mathbb{R}$, is given by

$$s(\boldsymbol{\eta}, \gamma) = 1 + s_0 \cos(m_S \vartheta - 2\pi\gamma), \tag{3.4}$$

where $\vartheta := \arctan(\eta_2/\eta_1)$, $0 \leq s_0 < 1$ denotes the amplitude of the anisotropy of the interfacial free energy, and m_S is the symmetry index. We note that ϑ is related to the inclination of the normal vector of the interface in the laboratory frame. The function $g(\eta)$ is the quartic double-well function

$$g(\eta) = \frac{1}{4}\,\eta^2\,(1-\eta)^2, \quad \eta \in \mathbb{R}, \tag{3.5}$$

For polycrystallization without orientational mismatch the orientational free energy density is given by

$$f_{ori}(\omega(\phi), \nabla\Theta) = 2\pi\xi_0\omega(\phi)|\nabla\Theta|, \tag{3.6}$$

where $\xi_0 > 0$ stands for the correlation length of the orientational field. Moreover, $H > 0$ in (3.1) refers to the free energy of the low-grain boundaries.

In case of polycrystallization with orientational mismatch we use an orientational free energy from [16] which is given by (cf. Fig. 1)

$$f_{ori}(\omega(\phi), \nabla\Theta) \; = \tag{3.7}$$
$$\begin{cases} b_1\,|\nabla\Theta| & , \; \xi_0|\nabla\Theta| \leq \frac{1}{2r_1}, \\ a_2 + b_2\,(|\nabla\Theta| - \frac{1}{2r_1}\xi_0^{-1}) & , \; \frac{1}{2r_1} \leq \xi_0|\nabla\Theta| \leq \frac{\delta+1/2}{2(\delta r_1+(1-\delta)r_2)}, \\ a_3 + b_3(|\nabla\Theta| - \frac{\delta+1/2}{2(\delta r_1+(1-\delta)r_2)}\xi_0^{-1}) & , \; \xi_0|\nabla\Theta| \geq \frac{\delta+1/2}{2(\delta r_1+(1-\delta)r_2)}, \end{cases}$$

where $\delta \in (0, 1)$, $0 < r_2 < r_1$, and

$$b_1 := 2(1-\delta)\pi\xi_0\omega(\phi)r_2,$$
$$a_2 := (1-\delta)\pi\omega(\phi)\frac{r_2}{r_1}, \quad b_2 := 2\pi\xi_0\omega(\phi)\frac{(1/2-(1-\delta)r_2/r_1)r_1(\delta r_1+(1-\delta)r_2)}{r_1/2-(1-\delta)r_2},$$
$$a_3 := \pi\omega(\phi)/2, \quad b_3 := 2\pi r_1\xi_0\omega(\phi).$$

For a derivation of (3.7) we refer to [4].

The orientational free energy density $f_{ori}(\omega(\phi), \nabla\Theta)$ is not differentiable in the classical sense, but admits a subdifferential

$$\partial_{\nabla\Theta} f_{ori}(\omega(\phi), \nabla\Theta) = (\partial_{\partial\Theta/\partial x_1} f_{ori}(\omega(\phi), \nabla\Theta), \partial_{\partial\Theta/\partial x_2} f_{ori}(\omega(\phi), \nabla\Theta))^T. \tag{3.8}$$

For f_{ori} given by (3.6) the subdifferential reads as follows:

$$\partial_{\partial\Theta/\partial x_i} f_{ori}(\omega(\phi), \nabla\Theta) = \begin{matrix} [-b, +b] \\ \operatorname{sgn}(\partial\Theta/\partial x_i)\, b \end{matrix} \begin{matrix} , \nabla\Theta = \mathbf{0} \\ , \nabla\Theta \neq \mathbf{0} \end{matrix}, \quad 1 \leq i \leq 2, \tag{3.9}$$

where $b := 2\pi\xi_0\omega(\phi)$.

On the other hand, if f_{ori} is defined by (3.7), the components $\partial_{\partial\Theta/\partial x_i} f_{ori}(\omega(\phi), \nabla\Theta)$, $1 \le i \le 2$, of the subdifferential $\partial_{\nabla\Theta} f_{ori}(\omega(\phi), \nabla\Theta)$ are given by

$$\partial_{\partial\Theta/\partial x_i} f_{ori}(\omega(\phi), \nabla\Theta) = \begin{cases} [-b_1, +b_1] & , \ \nabla\Theta = \mathbf{0} \\ \operatorname{sgn}(\partial\Theta/\partial x_i)\, b_1 & , \ 0 < |\nabla\Theta| < \frac{1}{2r_1}\xi_0^{-1} \\ \operatorname{sgn}(\partial\Theta/\partial x_i)\, [b_1, b_2] & , \ |\nabla\Theta| = \frac{1}{2r_1}\xi_0^{-1} \\ \operatorname{sgn}(\partial\Theta/\partial x_i)\, b_2 & , \ \frac{1}{2r_1}\xi_0^{-1} < |\nabla\Theta| < \frac{1}{2r_1}\xi_0^{-1} \\ \operatorname{sgn}(\partial\Theta/\partial x_i)\, [b_2, b_3] & , \ |\nabla\Theta| = \frac{1}{r_1+r_2}\xi_0^{-1} \\ \operatorname{sgn}(\partial\Theta/\partial x_i)\, b_3 & , \ \frac{1}{r_1+r_2}\xi_0^{-1} < |\nabla\Theta| \end{cases} . \tag{3.10}$$

Likewise, the associated free energy $F(\phi, \Theta)$ is not Gâteaux differentiable in Θ. We set

$$F(\phi, \Theta) := F_1(\phi, \Theta) + F_2(\phi, \Theta), \tag{3.11}$$

$$F_1(\phi, \Theta) := \frac{1}{2}\int_\Omega s(\nabla\phi, \Theta)^2\, |\nabla\phi|^2\, dx + \int_\Omega g(\phi)\, dx,$$

$$F_2(\phi, \Theta) := \frac{H}{2\xi_0}\int_\Omega f_{ori}(\omega(\phi), \nabla\Theta)\, dx. \tag{3.12}$$

The functional $F_2(\phi, \Theta)$ admits a subdifferential $\partial_\Theta F_2(\phi, \Theta)$ given by

$$\partial_\Theta F_2(\phi, \Theta) = \frac{H}{2\xi_0}\left\{-\nabla\cdot\mathbf{q} \mid \mathbf{q} \in \partial_{\nabla\Theta} f_{ori}(\omega(\phi), \nabla\Theta)\frac{\nabla\Theta}{|\nabla\Theta|}\right\}. \tag{3.13}$$

The functional $F_1(\phi, \Theta)$ is Gâteaux differentiable in Θ with Gâteaux derivative

$$\frac{\delta F_1(\phi, \Theta)}{\delta\Theta} = s(\nabla\phi, \Theta)\frac{\partial s(\nabla\phi, \Theta)}{\partial\Theta}|\nabla\phi|^2. \tag{3.14}$$

For practical purposes we replace $\partial_{\nabla\Theta} f_{ori}(\omega(\phi), \nabla\Theta)$ by its Moreau–Yosida approximation $\partial_{\nabla\Theta,\lambda} f_{ori}(\omega(\phi), \nabla\Theta)$ with regularization parameter $0 < \lambda \ll 1$ (cf., e.g., [17]). Then $F_2(\phi, \Theta)$ is Gâteaux differentiable in Θ with Gâteaux derivative

$$\frac{\delta F_2(\phi, \Theta)}{\delta\Theta} = \frac{H}{2\xi_0}\left\{-\nabla\cdot\partial_{\nabla\Theta,\lambda} f_{ori}(\omega(\phi), \nabla\Theta)\frac{\nabla\Theta}{|\nabla\Theta|}\right\}. \tag{3.15}$$

The functionals $F_i(\Theta, \phi)$, $1 \le i \le 2$, are Gâteaux differentiable in ϕ with Gâteaux derivatives

$$\frac{\delta F_1(\phi, \Theta)}{\delta\phi} = -\nabla\cdot(\mathbb{A}(\nabla\phi, \Theta)\nabla\phi), \tag{3.16}$$

$$\frac{\delta F_2(\phi, \Theta)}{\delta\phi} = \frac{H}{2\xi_0}\frac{\partial f_{ori}(\omega(\phi), \nabla\Theta)}{\partial\omega(\phi)}\omega_\phi(\phi) + g_\phi(\phi),$$

where the 2×2 matrix $\mathbb{A}(\boldsymbol{\eta}, \gamma) = (a_{ij}(\boldsymbol{\eta}, \gamma))_{i,j=1}^2$, $\boldsymbol{\eta} \in \mathbb{R}^2$, $\gamma \in \mathbb{R}$, is given by

$$a_{11}(\boldsymbol{\eta}, \gamma) = a_{22}(\boldsymbol{\eta}, \gamma) = s(\boldsymbol{\eta}, \gamma)^2, \tag{3.17}$$

$$a_{12}(\boldsymbol{\eta}, \gamma) = -a_{21}(\boldsymbol{\eta}, \gamma) = -s(\boldsymbol{\eta}, \gamma)\frac{\partial s(\boldsymbol{\eta}, \gamma)}{\partial\vartheta},$$

and $g_\phi(\phi)$ and $\omega_\phi(\phi)$ stand for the derivatives of $g(\phi)$ and $\omega(\phi)$ with respect to ϕ.

Denoting by $M_\phi > 0$ and $M_\Theta > 0$ the mobilities with respect to Θ and ϕ and specifying initial and boundary conditions, the dynamics of the spherulitic growth are described by the coupled system of evolutionary processes

$$\frac{\partial\phi}{\partial t} = M_\phi\left(-\frac{\delta F_2(\phi, \Theta)}{\delta\phi} + \frac{\delta F_1(\phi, \Theta)}{\delta\phi}\right) \quad \text{in } Q := \Omega\times(0, T), \tag{3.18a}$$

$$\phi = \phi_D \quad \text{on } \Sigma := \Gamma\times(0, T), \tag{3.18b}$$

$$\phi(0) = \phi_0 \quad \text{in } \Omega, \tag{3.18c}$$

and

$$\frac{\partial\Theta}{\partial t} = M_\Theta\left(-\frac{\delta F_1(\phi, \Theta)}{\delta\Theta} + \frac{\delta F_2(\phi, \Theta)}{\delta\Theta}\right), \quad \text{in } Q := \Omega\times(0, T), \tag{3.19a}$$

$$\Theta = \Theta_D \quad \text{on } \Sigma := \Gamma\times(0, T), \tag{3.19b}$$

$$\Theta(0) = \Theta_0 \quad \text{in } \Omega, \tag{3.19c}$$

where Θ_D, ϕ_D are given Dirichlet data on Γ and ϕ_0, Θ_0 are given initial configurations. We assume that

$$\Gamma = \bigcup_{i=1}^{\ell} \overline{\Gamma}_i, \quad \Gamma_i \cap \Gamma_j = \emptyset, \ i \neq j, \tag{3.20}$$

and

$$\phi_D|_{\Gamma_i} = \text{const.}, \ \Theta_D|_{\Gamma_i} = \text{const.}, \ 1 \leq i \leq \ell. \tag{3.21}$$

4. Discretization in time: the splitting scheme

We consider a discretization in time with respect to a partition of the time interval $[0, T]$ into subintervals $[t_{m-1}, t_m]$, $1 \leq m \leq M, M \in \mathbb{N}$, of length $\tau_m := t_m - t_{m-1}$. We denote by Θ^m and ϕ^m approximations of Θ and ϕ at time t_m and discretize the time derivatives in (3.18a) and (3.19a) by the backward difference quotient: Given Θ^{m-1} and ϕ^{m-1}, $1 \leq m < M$, compute Θ^m and ϕ^m such that

$$\phi^m - \phi^{m-1} = \tau_m M_\phi \Big(-\frac{\delta F_1(\phi^m, \Theta^m)}{\delta \phi} + \frac{\delta F_2(\phi^m, \Theta^m)}{\delta \phi} \quad \text{in } \Omega, \tag{4.1a}$$

$$\phi^m = \phi_D \quad \text{on } \Gamma, \tag{4.1b}$$

and

$$\Theta^m - \Theta^{m-1} = \tau_m M_\Theta \Big(-\frac{\delta F_2(\phi^m, \Theta^m)}{\delta \Theta} + \frac{\delta F_1(\phi^m, \Theta^m)}{\delta \Theta} \quad \text{in } \Omega, \tag{4.2a}$$

$$\Theta^m = \Theta_D \quad \text{on } \Gamma. \tag{4.2b}$$

As far as the first step of the splitting scheme is concerned, we consider the minimization problem

$$J_P^{(1)}(\phi^m) = \inf_{\phi \in V_1} J_P^{(1)}(\phi), \tag{4.3a}$$

where $V_1 := W^{1,2}_{\phi_D, \Gamma}(\Omega)$ and the objective functional $J_P^{(1)}$ is given by

$$J_P^{(1)}(\phi) = \frac{1}{2}\|\phi - \phi_h^{m-1}\|^2_{L^2(\Omega)} + \tag{4.3b}$$

$$\tau_m M_\phi \int_\Omega s(\nabla \phi_h^{m-1}, \Theta_h^{m-1})^2 |\nabla \phi|^2 \, dx + \tau_m M_\phi \ell_1^m(\phi),$$

where

$$\ell_1^m(\phi) := \int_\Omega f_{h,1}^m \phi \, dx, \quad f_{h,1}^m := \frac{\delta F_2(\phi_h^{m-1}, \Theta_h^{m-1})}{\delta \phi}, \tag{4.3c}$$

and $\phi_h^{m-1}, \Theta_h^{m-1}$ are some approximation of ϕ^{m-1} and Θ^{m-1} which will be specified in Section 5.

Theorem 4.1. *The minimization problem (4.3) has a unique solution $\phi^m \in V_1$.*

Proof. Let $\{\phi_n^m\}_{\mathbb{N}}$, $\phi_n^m \in V_1$, $n \in \mathbb{N}$, be a minimizing sequence, i.e.,

$$\lim_{\mathbb{N} \ni n \to \infty} J_P^{(1)}(\phi_n^m) = \inf_{\phi \in V_1} J_P^{(1)}(\phi). \tag{4.4}$$

An application of Young's inequality

$$ab \leq \varepsilon a^2 + \frac{1}{4\varepsilon} b^2, \quad a, b \in \mathbb{R}_+, \ \varepsilon > 0, \tag{4.5}$$

with $\varepsilon = 1/8$ yields

$$\frac{1}{2}\|\phi - \phi_h^{m-1}\|^2_{L^2(\Omega)} \geq \frac{1}{2}\|\phi\|^2_{L^2(\Omega)} + \frac{1}{2}\|\phi_h^{m-1}\|^2_{L^2(\Omega)} - \tag{4.6}$$

$$\|\phi\|_{L^2(\Omega)}\|\phi_h^{m-1}\|_{L^2(\Omega)} \geq \frac{3}{8}\|\phi\|^2_{L^2(\Omega)} - \frac{3}{2}\|\phi_h^{m-1}\|^2_{L^2(\Omega)}.$$

By another application of Young's inequality (4.5) with $\varepsilon = 1/(8\tau M_\phi)$ we obtain

$$|\tau M_\phi \ell_1^m(\phi)| \leq \frac{1}{8}\|\phi\|^2_{L^2(\Omega)} + 2\tau_m M_\phi \int_\Omega |f_{h,1}^m|^2 \, dx. \tag{4.7}$$

Observing (3.4) and (4.6), (4.7) it follows that

$$J_P^{(1)}(\phi) \geq \frac{1}{4}\,\|\phi\|^2_{L^2(\Omega)} + (1-s_0)^2\tau_m M_\phi \|\nabla\phi\|^2_{L^2(\Omega)} - \frac{3}{2}\|\phi_h^{m-1}\|^2_{L^2(\Omega)} - 2\tau_m M_\phi \int_\Omega |f_{h,1}^m|^2\,dx,$$

from which we deduce the coercivity of $J_P^{(1)}$. It follows that the minimizing sequence $\{\phi_n^m\}_{\mathbb{N}}$ is uniformly bounded. Consequently, there exist a subsequence $\mathbb{N}' \subset \mathbb{N}$ and a function $\phi^m \in V_1$ such that

$$\phi_n^m \rightharpoonup \phi^m \quad (\mathbb{N}' \ni n \to \infty) \text{ in } W^{1,2}(\Omega).$$

Since $J_P^{(1)}$ is convex and lower semicontinuous, it is weakly lower semicontinuous. We thus have

$$J_P^{(1)}(\phi^m) \leq \lim_{\mathbb{N}'\ni n\to\infty} \inf J_P^{(1)}(\phi_n^m),$$

and hence, in view of (4.9) we obtain

$$J_P^{(1)}(\phi^m) = \inf_{\phi\in V_1} J_P^{(1)}(\phi).$$

The uniqueness of ϕ^m follows from the strict convexity of $J_P^{(1)}$.

In the second step of the splitting scheme, we compute $\Theta^m \in V_2 := BV_{\Theta_D,\Gamma}(\Omega)$ as the solution of the minimization problem

$$J_P^{(2)}(\Theta^m) = \inf_{\Theta\in V_2} J_P^{(2)}(\Theta), \tag{4.8a}$$

where the objective functional $J_P^{(2)}$ is given by

$$J_P^{(2)}(\Theta) = \frac{1}{2}\|\Theta - \Theta_h^{m-1}\|^2_{L^2(\Omega)} + \frac{\tau_m M_\Theta H}{2\xi_0}\int_\Omega f_{ori}(\omega(\phi_h^{m-1}), D\Theta)\,dx + \tau_m M_\Theta \ell_2^m(\Theta), \tag{4.8b}$$

where

$$\ell_2^m(\Theta) := \int_\Omega f_{h,2}^m \Theta\,dx, \quad f_{h,2}^m := \frac{\delta F_1(\phi_h^m, \Theta_h^{m-1})}{\delta\Theta}\Theta\,dx. \tag{4.8c}$$

Theorem 4.2. *The minimization problem (4.8) has a solution $\Theta^m \in V_2$.*

Proof. Let $\{\Theta_n^m\}_{\mathbb{N}}$, $\Theta_n^m \in V_2$, $n \in \mathbb{N}$, be a minimizing sequence, i.e.,

$$\lim_{\mathbb{N}\ni n\to\infty} J_P^{(2)}(\Theta_n^m) = \inf_{\Theta\in V_2} J_P^{(2)}(\Theta). \tag{4.9}$$

As in the proof of Theorem 4.1, an application of Young's inequality yields

$$\frac{1}{2}\|\Theta - \Theta_h^{m-1}\|^2_{L^2(\Omega)} \geq \frac{3}{8}\|\Theta\|^2_{L^2(\Omega)} - \frac{3}{2}\|\Theta_h^{m-1}\|^2_{L^2(\Omega)}. \tag{4.10}$$

and

$$|\tau M_\Theta \ell_2^m(\Theta)| \leq \frac{1}{8}\|\Theta\|^2_{L^2(\Omega)} + 2\tau_m M_\Theta \int_\Omega |f_{h,2}^m|^2\,dx. \tag{4.11}$$

Observing (3.3), (3.6), (3.7), and (4.10), (4.11) it follows that

$$J_P^{(2)}(\Theta) \geq \frac{1}{4}\,\|\Theta\|^2_{L^2(\Omega)} + \tau_m M_\Theta \beta\,|D\Theta|(\Omega) - \frac{3}{2}\|\Theta^{m-1}\|^2_{L^2(\Omega)} - 2\tau_m M_\Theta \int_\Omega |f_{h,2}^m|^2\,dx,$$

where $\beta := \varepsilon_r$, if f_{ori} is given by (3.6), and $\beta := (1-\delta)\pi r_2 \varepsilon_r$ in case f_{ori} is given by (3.7). This implies the coercivity of $J_P^{(2)}$ on V_2. Hence, the minimizing sequence $\{\Theta_n^m\}_{\mathbb{N}}$ is uniformly bounded. Consequently, there exist a subsequence $\mathbb{N}' \subset \mathbb{N}$ and a function $\Theta^m \in V_2$ such that

$$\Theta_n^m \rightharpoonup^* \Theta^m \quad (\mathbb{N}' \ni n \to \infty) \text{ in } BV(\Omega).$$

The objective functional $J_P^{(2)}$ is weakly* lower semicontinuous in $BV(\Omega)$. We thus have

$$J_P^{(2)}(\Theta^m) \le \lim \inf_{\mathbb{N}' \ni n \to \infty} J_P^{(2)}(\Theta_n^m),$$

and hence, in view of (4.9) we obtain

$$J_P^{(2)}(\Theta^m) = \inf_{\Theta \in V_2} J_P^{(2)}(\Theta).$$

Remark 4.1. We note that the splitting scheme (4.3), (4.8) is different from those used in [3–5] where the first minimization problem is in Θ and the second one in ϕ. The reason for the reverse order is that for space adaptivity it is more advantageous to perform the adaptivity with respect to ϕ before the one for Θ. A more detailed explanation will be given in Section 6.

5. Discretization in space

Let $\mathcal{T}_h$ be a geometrically conforming, locally quasi-uniform, simplicial triangulation of the computational domain Ω. Given $D \subset \bar{\Omega}$, we denote by $\mathcal{N}_h(D)$ and $\mathcal{E}_h(D)$ the set of vertices and edges of $\mathcal{T}_h$ in D, and we refer to $P_k(D)$, $k \in \mathbb{N}$, as the set of polynomials of degree $\le k$ on D. Moreover, $h_K, K \in \mathcal{T}_h$, and h_E, $E \in \mathcal{E}_h$, stand for the diameter of K and the length of E, respectively. We define $h := \min\{h_K \mid K \in \mathcal{T}_h\}$. Due to the local quasi-uniformity of the triangulation there exist constants $0 < c_R \le C_R$ such that for all $K \in \mathcal{T}_h$ it holds

$$c_R h_K \le h_E \le C_R h_K, \quad E \in \mathcal{E}_h(\partial K). \tag{5.1}$$

For two quantities $a, b \in \mathbb{R}$ we will write $a \lesssim b$, if there exists a constant $C > 0$, independent of h, such that $a \le Cb$.

We will further use the following trace inequality (cf., e.g., [18]): There exists a constant $C_T > 0$, only depending on the polynomial degree k and the local geometry of the triangulation, such that for $v_h \in P_k(K)$ and $K \in \mathcal{T}_h$ it holds

$$\|v_h\|_{L^2(\partial K)} \le C_T h_K^{-1/2} \|v_h\|_{L^2(K)}. \tag{5.2}$$

For $E \in \mathcal{E}_h(\Omega)$, $E = K_+ \cap K_-$, $K_\pm \in \mathcal{T}_h(\Omega)$, and $v_h \in V_h$, we denote the average and jump of v_h across E by $\{v_h\}_E$ and $[v_h]_E$, i.e.,

$$\{v_h\}_E := \frac{1}{2}\ v_h|_{E\cap K_+} + v_h|_{E\cap K_-}\ , \quad [v_h]_E := v_h|_{E\cap K_+} - v_h|_{E\cap K_-},$$

whereas for $E \in \mathcal{E}_h(\Gamma)$ we set

$$\{v_h\}_E := v_h|_E, \quad [v_h]_E := v_h|_E.$$

The averages $\{\nabla v_h\}_E$, $\{\underline{\boldsymbol{\tau}}_h\}_E$ and jumps $[\nabla v_h]_E$, $[\underline{\boldsymbol{\tau}}_h]_E$ of vector-valued functions ∇v_h and $\underline{\boldsymbol{\tau}}_h$ are defined analogously. For $E \in \mathcal{E}_h(\Omega)$ it holds

$$\int_E u_h\ v_h\ ds = \int_E \{u_h\}_E\ [v_h]_E + [u_h]_E\ \{v_h\}_E \quad ds. \tag{5.3}$$

We further denote by $\mathbf{n}_E$, $E \in \mathcal{E}_h(\Omega)$, with $E = K_+ \cap K_-$ the unit normal on E pointing from K_+ to K_- and by $\mathbf{n}_E$, $E \in \mathcal{E}_h(\Gamma)$, the exterior unit normal on E.

We consider the finite element approximation with the DG spaces

$$V_{h,\phi_D,\Gamma}^{(1)} := \{v_h \in C(\bar{\Omega}) \to \mathbb{R} \mid v_h|_K \in P_1(K),\ K \in \mathcal{T}_h,\ v_h|_E = \phi_D,\ E \in \mathcal{E}_h(\Gamma)\}, \tag{5.4a}$$

$$V_{h,0,\Gamma}^{(1)} := \{v_h \in C(\bar{\Omega}) \to \mathbb{R} \mid v_h|_K \in P_1(K),\ K \in \mathcal{T}_h,\ v_h|_E = 0,\ E \in \mathcal{E}_h(\Gamma)\}, \tag{5.4b}$$

$$V_{h,\Theta_D,\Gamma}^{(2)} := \{v_h : \bar{\Omega} \to \mathbb{R} \mid v_h|_K \in P_1(K),\ K \in \mathcal{T}_h,\ v_h|_E = \Theta_D,\ E \in \mathcal{E}_h(\Gamma)\}, \tag{5.4c}$$

$$V_{h,0,\Gamma}^{(2)} := \{v_h : \bar{\Omega} \to \mathbb{R} \mid v_h|_K \in P_1(K),\ K \in \mathcal{T}_h,\ v_h|_E = 0,\ E \in \mathcal{E}_h(\Gamma)\}, \tag{5.4d}$$

$$\mathbf{RT}_0(\Omega;\mathcal{T}_h) := \{\underline{\mathbf{q}}_h \in \underline{\mathbf{H}}(\mathrm{div};\Omega) \mid \underline{\mathbf{q}}_h|_K \in \mathbf{RT}_0(K), K \in \mathcal{T}_h\}, \tag{5.4e}$$

$$\underline{\mathbf{V}}_h := \{\underline{\mathbf{q}}_h : \bar{\Omega} \to \mathbb{R}^2 \mid \underline{\mathbf{q}}_h|_K \in \mathbf{RT}_0(K),\ K \in \mathcal{T}_h\}, \tag{5.4f}$$

where $\mathbf{RT}_0(K) := P_0(K)^2 + xP_0(K)$ stands for the lowest order Raviart–Thomas element. We note that $V_{h,\phi_D,\Gamma}^{(1)} \subset W_{\phi_d,\Gamma}^{1,2}(\Omega)$ and $V_{h,0,\Gamma}^{(1)} \subset W_{0,\Gamma}^{1,2}(\Omega)$. Moreover, for $\underline{\mathbf{q}}_h \in \underline{\mathbf{V}}_h$, we have $(\nabla \cdot \underline{\mathbf{q}}_h)|_K \in P_0(K), K \in \mathcal{T}_h$, and $\mathbf{n}_E \cdot \underline{\mathbf{q}}_h|_E \in P_0(E), E \in \mathcal{E}_h(\Gamma)$.

For $u_h \in V_{h,\Theta_D,\Gamma}^{(2)}$ and $u_h \in V_{h,0,\Gamma}^{(2)}$ we define the broken gradient $\nabla_h u_h$ by means of

$$\nabla_h u_h|_K := \nabla u_h|_K, \quad K \in \mathcal{T}_h. \tag{5.5}$$

Following [19,20], we define a recovery operator $\underline{\mathbf{R}}_h : V_{h,\Theta_D,\Gamma}^{(2)} \to \underline{\mathbf{V}}_h$ resp. $\underline{\mathbf{R}}_h : V_{h,0,\Gamma}^{(2)} \to \underline{\mathbf{V}}_h$ according to

$$\int_\Omega \underline{\mathbf{R}}_h(u_h) \cdot \underline{\mathbf{q}}_h\ dx = \sum_{E \in \mathcal{E}_h(\Omega)} \int_E [u_h]_E\ \mathbf{n}_E \cdot \{\underline{\mathbf{q}}_h\}_E\ ds, \quad \underline{\mathbf{q}}_h \in \underline{\mathbf{V}}_h. \tag{5.6}$$

We define the broken DG gradient $\nabla_{DG} u_h$ as follows:

$$\nabla_{DG} u_h := \nabla_h u_h - \underline{\mathbf{R}}_h(u_h). \tag{5.7}$$

The following auxiliary result from [19] will enable us to estimate the L^1 norm of $\underline{\mathbf{R}}_h(u_h)$ for $u_h \in V^{(2)}_{h,\Theta_D,\Gamma}$ resp. $u_h \in V^{(2)}_{h,0,\Gamma}$ (cf. Lemma A2 in [19]).

Lemma 5.1. *There exists a constant $C_{IS} > 0$, independent of h, such that for $u_h \in V^{(2)}_h$ ($V^{(2)}_h = V^{(2)}_{h,\Theta_D,\Gamma}$ or $V^{(2)}_h = V^{(2)}_{h,0,\Gamma}$) it holds*

$$\inf_{u_h \in V^{(2)}_h} \sup_{\underline{\mathbf{q}}_h \in \underline{\mathbf{V}}^{(2)}_h} \frac{\int_\Omega \underline{\mathbf{R}}_h(u_h) \cdot \underline{\mathbf{q}}_h \, dx}{\|u_h\|_{L^1(\Omega)} \|\underline{\mathbf{q}}_h\|_{L^\infty(\Omega;\mathbb{R}^2)}} \geq C_{IS}. \tag{5.8}$$

Theorem 5.1. *Under the assumptions of Lemma 5.1 there exists a constant $C_{rec} > 0$, independent of h, such that for $u_h \in V^{(2)}_h$ it holds*

$$\|\underline{\mathbf{R}}_h(u_h)\|_{L^1(\Omega;\mathbb{R}^2)} \leq C_{rec} \sum_{E \in \mathcal{E}_h(\Omega)} \int_E |[u_h]_E| \, ds. \tag{5.9}$$

Proof. We have

$$\begin{aligned} \|\underline{\mathbf{R}}_h(u_h)\|_{L^1(\Omega;\mathbb{R}^2)} &= \sup_{\underline{\mathbf{q}} \in L^\infty(\Omega;\mathbb{R}^2)} \frac{\int_\Omega \underline{\mathbf{R}}_h(u_h) \cdot \underline{\mathbf{q}} \, dx}{\|\underline{\mathbf{q}}\|_{L^\infty(\Omega;\mathbb{R}^2)}} \\ &\geq \sup_{\underline{\mathbf{q}}_h \in \underline{\mathbf{V}}_h} \frac{\int_\Omega \underline{\mathbf{R}}_h(u_h) \cdot \underline{\mathbf{q}}_h \, dx}{\|\underline{\mathbf{q}}_h\|_{L^\infty(\Omega;\mathbb{R}^2)}}. \end{aligned} \tag{5.10}$$

The inf-sup property (5.8) implies

$$\|\underline{\mathbf{R}}_h(u_h)\|_{L^1(\Omega;\mathbb{R}^2)} \leq C_{IS}^{-1} \sup_{\underline{\mathbf{q}}_h \in \underline{\mathbf{V}}_h} \frac{\int_\Omega \underline{\mathbf{R}}_h(u_h) \cdot \underline{\mathbf{q}}_h \, dx}{\|\underline{\mathbf{q}}_h\|_{L^\infty(\Omega;\mathbb{R}^2)}}. \tag{5.11}$$

Now, observing (5.6), for $E \in \mathcal{E}_h(\Omega)$ we obtain

$$\begin{aligned} &\int_\Omega \underline{\mathbf{R}}_h(u_h) \cdot \underline{\mathbf{q}}_h \, dx \leq \\ &\sum_{E \in \mathcal{E}_h(\Omega)} \int_E |[u_h]_E| \, |\{\underline{\mathbf{q}}_h\}_E| \, ds \leq \\ &\frac{1}{2} \sum_{E \in \mathcal{E}_h(\Omega)} \int_E |[u_h]_E| \, |\underline{\mathbf{q}}_h|_{E_+} + \underline{\mathbf{q}}_h|_{E_-}|^q \, ds \leq \\ &\|\underline{\mathbf{q}}_h\|_{L^\infty(\Omega;\mathbb{R}^2)} \sum_{E \in \mathcal{E}_h(\Omega)} \int_E |[u_h]_E| \, ds. \end{aligned} \tag{5.12}$$

Using (5.12) in (5.11) gives (5.9).

The fully discrete splitting scheme reads as follows:
Given $(\phi_h^{m-1}, \Theta_h^{m-1}) \in V^{(1)}_{h,\phi_D,\Gamma} \times V^{(2)}_{h,\Theta_D,\Gamma}$, first find $\phi_h^m \in V^{(1)}_{h,\phi_D,\Gamma}$ as the solution of the minimization problem

$$J_P^{(1)}(\phi_h^m) = \inf_{\phi_h \in V^{(1)}_{h,\phi_D,\Gamma}} J_P^{(1)}(\phi_h). \tag{5.13}$$

Since $V^{(1)}_{h,\phi_D,\Gamma}$ is a closed subspace of $W^{1,2}_{\phi_D,\Gamma}(\Omega)$, the existence and uniqueness of a solution of (5.13) follows as in Theorem 4.1.

In the second step of the splitting scheme, we compute $\Theta_h^m \in V^{(2)}_{h,\Theta_D,\Gamma}$ as the solution of the minimization problem

$$J^{(2)}_{h,P}(\Theta_h^m) = \inf_{\Theta_h \in V^{(2)}_{h,\Theta_D,\Gamma}} J^{(2)}_{h,P}(\Theta_h), \tag{5.14a}$$

where the objective functional $J^{(2)}_{h,P}$ is given by

$$J^{(2)}_{h,P}(\Theta_h) = \frac{1}{2}\|\Theta_h - \Theta_h^{m-1}\|^2_{L^2(\Omega)} + \frac{\tau_m M_\Theta H}{2\xi_0}\int_\Omega f_{ori}(\omega(\phi_h^m), \nabla_{DG}\Theta_h)\,dx\ + \tag{5.14b}$$
$$\tau_m M_\Theta \ell_2^m(\Theta_h) + \alpha_1 \sum_{E\in\mathcal{E}_h(\Omega)}\int_E |[\Theta_h]_E|\,ds,$$

and $\alpha_1 > 0$ is a penalty parameter.

Theorem 5.2. *For sufficiently large penalty parameter $\alpha_1 > 0$, the minimization (5.14) has a solution $\Theta_h^m \in V^{(2)}_{h,\Theta_D,\Gamma}$.*

Proof. We show that the objective functional $J^{(2)}_{h,P}$ is coercive on $V^{(2)}_{h,\Theta_D,\Gamma}$ equipped with the norm of $W^{1,1}(\Omega;\mathcal{T}_h)$. As in the proof of Theorem 4.2 we have

$$\frac{1}{2}\|\Theta_h - \Theta_h^{m-1}\|^2_{L^2(\Omega)} \geq \frac{3}{8}\|\Theta_h\|^2_{L^2(\Omega)} - \frac{3}{2}\|\Theta_h^{m-1}\|^2_{L^2(\Omega)}, \tag{5.15a}$$
$$|\tau M_{\Theta_h}\ell_2^m(\Theta)| \leq \frac{1}{8}\|\Theta_h\|^2_{L^2(\Omega)} + 2\tau_m M_\Theta \int_\Omega |f^m_{h,2}|^2\,dx. \tag{5.15b}$$

Observing (3.3), (3.6), (3.7), and (5.7), (5.9), as well as (5.15), it follows that

$$J^{(2)}_{h,P}(\Theta_h) \geq \frac{1}{4}\ \|\Theta\|^2_{L^2(\Omega)} + \tau_m M_\Theta H\beta\ |\nabla\Theta_h|(\Omega) +$$
$$(\alpha_1 - \frac{\tau_m M_\Theta H}{2\xi_0}\gamma)\sum_{E\in\mathcal{E}_h(\Omega)}\int_E |[\Theta_h]_E|\,ds -$$
$$\frac{3}{2}\|\Theta_h^{m-1}\|^2_{L^2(\Omega)} - 2\tau_m M_\Theta\int_\Omega |f^m_{h,2}|^2\,dx,$$

where β as in the proof of Theorem 4.2 and $\gamma := 2\pi\xi_0(1-\varepsilon_r)$, if f_{ori} is given by (3.6), and $\gamma := 2\pi r_1\xi_0(1-\varepsilon_r)C_{rec}$ in case f_{ori} is given by (3.7). This implies coercivity for sufficiently large α_1.

In view of $J^{(2)}_{h,P}$ being continuous, convex, and coercive and $V^{(2)}_{h,\Theta_D,\Gamma}$ being finite dimensional, the assertion follows from a standard minimizing sequence argument.

The necessary and sufficient optimality condition for (5.13) amounts to the computation of $\phi_h^m \in V^{(1)}_{h,\phi_D,\Gamma}$ such that for all $v_h \in V^{(1)}_{h,0,\Gamma}$ it holds

$$\int_\Omega \phi_h^m v_h\,dx + \tau_m M_\phi\int_\Omega s(\nabla\phi_h^{m-1},\Theta_h^{m-1})^2\nabla\phi_h^m\cdot\nabla v_h\,dx\ = \tag{5.16}$$
$$\int_\Omega \phi_h^{m-1}v_h\,dx + \tau_m M_\phi \ell_1^m(v_h).$$

For the construction of the equilibrated a posteriori error estimator in Section 6 we consider the mixed formulation of (5.16): Find $(\tilde\phi_h^m, \underline{\mathbf{p}}^m_{h,1}) \in V^{(1)}_{h,\phi_D,\Gamma}\times \mathrm{RT}_0(\Omega;\mathcal{T}_h)$ such that for all $(v_h, \underline{\mathbf{q}}_h) \in V^{(1)}_{h,0,\Gamma}\times\mathrm{RT}_0(\Omega;\mathcal{T}_h)$ it holds

$$\int_\Omega s(\nabla\phi_h^{m-1},\Theta_h^{m-1})\underline{\mathbf{p}}^m_{h,1}\cdot\underline{\mathbf{q}}_h\,dx = -\int_\Omega \tilde\phi_h^m\nabla\cdot(s(\nabla\phi_h^{m-1},\Theta_h^{m-1})\underline{\mathbf{q}}_h)\,dx\ + \tag{5.17a}$$
$$\int_\Gamma \phi_D\mathbf{n}_\Gamma\cdot s(\nabla\phi_h^{m-1},\Theta_h^{m-1})^2\underline{\mathbf{q}}_h\,ds,$$
$$\int_\Omega \tilde\phi_h^m v_h\,dx - \tau_m M_\phi\int_\Omega \nabla\cdot(s(\nabla\phi_h^{m-1},\Theta_h^{m-1})\underline{\mathbf{p}}^m_{h,1})v_h\,dx\ = \tag{5.17b}$$
$$\int_\Omega \phi_h^{m-1}v_h\,dx + \tau_m M_\phi\int_\Omega f^m_{h,1}v_h\,dx. \tag{5.17c}$$

On the other hand, replacing $\partial_{\nabla\Theta}f_{ori}(\omega(\phi_h^m),\nabla\Theta_h^m)$ by its Moreau–Yosida approximation $a(\phi^m,\Theta^m) := \partial_{\nabla\Theta,\lambda}f_{ori}(\omega(\phi_h^m),\nabla\Theta_h^m)$, the necessary and sufficient optimality condition for (5.14) leads to an IPDG approximation, namely the computation of $\Theta_h^m \in V^{(2)}_{h,\Theta_D,\Gamma}$ such that for all $v_h \in V^{(2)}_{h,0,\Gamma}$ it holds

$$\int_\Omega \Theta_h^m v_h\,dx + a_h^{DG}(\Theta_h^m, v_h) = \int_\Omega \Theta_h^{m-1}v_h\,dx + \tau M_\Theta\ell_2^m(v_h), \tag{5.18a}$$

where the semilinear form $a_h^{DG}(\cdot,\cdot)$ is given by

$$a_h^{DG}(\Theta_h^m, v_h) := \frac{\tau_m M_\Theta H}{2\xi_0} \sum_{K\in\mathcal{T}_h} \int_K a(\phi^m, \Theta^m) \frac{\nabla_{DG}\Theta_h^m}{|\nabla_{DG}\Theta_h^m|} \cdot \nabla_{DG} v_h \, dx \, + \tag{5.18b}$$

$$\alpha_1 \sum_{E\in\mathcal{E}_h(\Omega)} \int_E \frac{[\Theta_h^m]_E}{|[\Theta_h^m]_E|} [v_h]_E \, ds.$$

In view of (5.6) and (5.7) we obtain

$$a_h^{DG}(\Theta_h^m, v_h) := \tau M_\phi \sum_{K\in\mathcal{T}_h} \int_K a(\phi^m, \Theta^m) |\nabla_{DG}\Theta_h^m|^{-1} \nabla_{DG}\Theta_h^m \cdot \tag{5.19}$$

$$(\nabla v_h - \underline{\mathbf{R}}_h(v_h)) \, dx + \alpha_1 \sum_{E\in\mathcal{E}_h(\Omega)} \int_E \frac{[\Theta_h^m]_E}{|[\Theta_h^m]_E|} [v_h]_E \, ds \, =$$

$$\tau M_\phi \sum_{K\in\mathcal{T}_h} \int_K a(\phi^m, \Theta^m) |\nabla_{DG}\Theta_h^m|^{-1} \nabla_{DG}\Theta_h^m \cdot \nabla v_h \, dx \, -$$

$$\sum_{E\in\mathcal{E}_h(\Omega)} \int_E [v_h]_E \, \mathbf{n}_E \cdot \{a(\phi^m, \Theta^m) |\nabla_{DG}\Theta_h^m|^{-1} \nabla_{DG}\Theta_h^m\}_E \, ds \, +$$

$$\alpha_1 \sum_{E\in\mathcal{E}_h(\Omega)} \int_E \frac{[\Theta_h^m]_E}{|[\Theta_h^m]_E|} [v_h]_E \, ds.$$

We will consider a two-field formulation of the IPDG approximation (5.18). To this end we set

$$\underline{\mathbf{p}}_{h,2}^m = a(\phi^m, \Theta^m) |\nabla_{DG}\Theta_h^m|^{-1} \nabla_{DG}\Theta_h^m, \tag{5.20a}$$

$$\Theta_h^m - \frac{\tau_m M_\Theta H}{2\xi_0} \nabla \cdot \underline{\mathbf{p}}_{h,2}^m = \Theta_h^{m-1} + \tau_m M_\Theta f_{h,2}^m. \tag{5.20b}$$

Multiplying (5.20a) by $\underline{\mathbf{q}}_h \in \underline{\mathbf{V}}_h$, integrating over $K \in \mathcal{T}_h$, and summing over all K yields

$$\sum_{K\in\mathcal{T}_h} \int_K \underline{\mathbf{p}}_{h,2}^m \cdot \underline{\mathbf{q}}_h \, dx = \sum_{K\in\mathcal{T}_h} \int_K a(\phi^m, \Theta^m) |\nabla_{DG}\Theta_h^m|^{-1} \nabla_{DG}\Theta_h^m \cdot \underline{\mathbf{q}}_h \, dx. \tag{5.21a}$$

Moreover, multiplying (5.20b) by $v_h \in V_{h,0,\Gamma}^{(2)}$, integrating over $K \in \mathcal{T}_h$, summing over all K, and applying Green's formula elementwise, we get

$$\sum_{K\in\mathcal{T}_h} \int_K \Theta_h^m v_h \, dx - \frac{\tau_m M_\Theta H}{2\xi_0} \sum_{K\in\mathcal{T}_h} \int_K \nabla \cdot \underline{\mathbf{p}}_{h,2}^m v_h \, dx = \sum_{K\in\mathcal{T}_h} \int_K \Theta_h^m v_h \, dx \, + \tag{5.21b}$$

$$\frac{\tau_m M_\Theta H}{2\xi_0} \sum_{K\in\mathcal{T}_h} \int_K \underline{\mathbf{p}}_{h,2}^m \cdot \nabla v_h \, dx - \frac{\tau_m M_\Theta H}{2\xi_0} \sum_{K\in\mathcal{T}_h} \int_{\partial K} \mathbf{n}_{\partial K} \cdot \underline{\mathbf{p}}_{h,2}^m v_h \, ds \, =$$

$$\sum_{K\in\mathcal{T}_h} \int_K \Theta_h^{m-1} v_h \, dx + \tau_m M_\Theta \sum_{K\in\mathcal{T}_h} \int_K f_{h,2}^m v_h \, dx.$$

Replacing $\underline{\mathbf{p}}_{h,2}^m|_{\partial K}$ with some numerical flux function $\hat{\underline{\mathbf{p}}}_{\partial K}^m$, we obtain the following two-field formulation of a general DG approximation of the Θ-equation: Find $(\Theta_h^m, \underline{\mathbf{p}}_{h,2}^m) \in V_{h,\Theta_D,\Gamma}^{(2)} \times \underline{\mathbf{V}}_h$ such that for all $(v_h, \underline{\mathbf{q}}_h) \in V_{h,0,\Gamma}^{(2)} \times \underline{\mathbf{V}}_h$ it holds

$$\sum_{K\in\mathcal{T}_h} \int_K \underline{\mathbf{p}}_{h,2}^m \cdot \underline{\mathbf{q}}_h \, dx = \sum_{K\in\mathcal{T}_h} \int_K a(\phi^m, \Theta^m) |\nabla_{DG}\Theta_h^m|^{-1} \nabla_{DG}\Theta_h^m \cdot \underline{\mathbf{q}}_h \, dx, \tag{5.22a}$$

$$\sum_{K\in\mathcal{T}_h} \int_K \Theta_h^m v_h \, dx + \frac{\tau_m M_\Theta H}{2\xi_0} \sum_{K\in\mathcal{T}_h} \int_K \underline{\mathbf{p}}_{h,2}^m \cdot \nabla v_h \, dx \, - \tag{5.22b}$$

$$\frac{\tau_m M_\Theta H}{2\xi_0} \sum_{K\in\mathcal{T}_h} \int_{\partial K} \mathbf{n}_{\partial K} \cdot \hat{\underline{\mathbf{p}}}_{\partial K}^m v_h \, ds = \sum_{K\in\mathcal{T}_h} \int_K \Theta_h^{m-1} v_h \, dx \, +$$

$$\tau_m M_\Theta \sum_{K\in\mathcal{T}_h} \int_K f_{h,2}^m v_h \, dx.$$

In particular, if the numerical flux function $\hat{\underline{\mathbf{p}}}^m_{\partial K}|_E$, $E \in \mathcal{E}_h(\bar{\Omega})$ is chosen according to

$$\hat{\underline{\mathbf{p}}}^m_{\partial K}|_E := \{a(\phi^m, \Theta^m_h)|\nabla\Theta^m_h|^{-1}\nabla\Theta^m_h\}_E - \alpha_1|[\Theta^m_h]_E|^{-1}[\Theta^m_h]_E\ \mathbf{n}_E, \tag{5.23}$$

we recover the IPDG approximation (5.18) by eliminating $\underline{\mathbf{p}}^m_{h,2}$ from (5.22).

6. Equilibrated a posteriori error estimators

Given Banach spaces V, Q with norms $\|\cdot\|_V, \|\cdot\|_Q$, a convex and coercive objective functional $J_P : V \to \mathbb{R}$, we consider the minimization problems

$$\inf_{u\in V} J_P(u) \tag{6.1}$$

and

$$\inf_{q\in Q} J_D(q), \tag{6.2}$$

where $J_D : Q \to \mathbb{R}$ is the Fenchel conjugate of J_P. An abstract approach to the a posteriori error control for (6.1) has been provided in [21] (cf. also [22]):

Given some approximation $v \in V$ of the minimizer u of (6.1), the a posteriori error estimate from [21] states that for any admissible function $q \in Q$ it holds

$$\|u - v\|^2_V \lesssim J_P(v) + J_D(q). \tag{6.3}$$

6.1. A posteriori error estimator for the ϕ-equation

We apply (6.3) with $V = W^{1,2}_{\phi_D,\Gamma}(\Omega)$, $Q = \underline{\mathbf{H}}(\mathrm{div};\Omega)$, $J_P = J^{(1)}_P$, and $v = \phi^m_h$, $q = \underline{\mathbf{p}}^m_{h,1}$. Following Example 3.2 in [22], for the Fenchel dual we obtain

$$J^{(1)}_D(\underline{\mathbf{p}}^m_{h,1}) = \frac{1}{2}\tau M_\phi \int_\Omega |\underline{\mathbf{p}}^m_{h,1}|^2\, dx - \tau M_\phi \int_\Gamma \phi_D \mathbf{n}_\Gamma \cdot (s(\nabla\phi^{m-1}_h, \Theta^{m-1}_h)\underline{\mathbf{p}}^m_{h,1})\, ds + \tag{6.4}$$
$$\frac{1}{2}\|\tau_m M_\phi \nabla\cdot(s(\nabla\phi^{m-1}_h, \Theta^{m-1}_h)\underline{\mathbf{p}}^m_{h,1}) + \phi^{m-1}_h + \tau_m M_\phi f^m_{h,1}\|^2_{L^2(\Omega)} - \frac{1}{2}\|\phi^{m-1}_h\|^2_{L^2(\Omega)}.$$

We thus obtain

$$\|\phi^m - \phi^m_h\|^2_{W^{1,2}(\Omega)} \lesssim J^{(1)}_P(\phi^m_h) + J^{(1)}_D(\underline{\mathbf{p}}^m_{h,1}). \tag{6.5}$$

Referring to $\Pi^{(0)}_h$ as the L^2 projection onto $V^{(0)}_h := \{v_h : \bar{\Omega} \to \mathbb{R} \mid v_h|_K \in P_0(K), K \in \mathcal{T}_h\}$, we note that the flux function $\underline{\mathbf{p}}^m_{h,1}$ is equilibrated in the sense that

$$\Pi^{(0)}_h(\phi^m_h) - \tau_m M_\phi \Pi^{(0)}_h(\nabla(s(\nabla\phi^{m-1}_h, \Theta^{m-1}_h)\underline{\mathbf{p}}^m_{h,1})) = \tag{6.6}$$
$$\Pi^{(0)}_h(\phi^{m-1}_h) + \tau_m M_\phi \Pi^{(0)}_h(f^m_{h,1}) \text{ in each } K \in \mathcal{T}_h,$$

as follows from (5.17b) with $v_h|_K = p_0 \in P_0(K)$ and $v_h|_{K'} = 0, K' \neq K$.

Moreover, taking (6.6) into account, we have

$$\frac{1}{2}\|\phi^m_h - \phi^{m-1}_h\|^2_{L^2(\Omega)} + \frac{1}{2}\,\|\,\tau_m M_\phi \nabla\cdot(s(\nabla\phi^{m-1}_h, \Theta^{m-1}_h)\underline{\mathbf{p}}^m_{h,1}) + \phi^{m-1}_h + \tag{6.7}$$
$$\tau_m M_\phi f^m_{h,1}\,\|^2_{L^2(\Omega)} - \frac{1}{2}\|\phi^{m-1}_h\|^2_{L^2(\Omega)} - \tau_m M_\phi \int_\Omega f^m_{h,1}\phi^m_h\, dx =$$
$$\tau_m M_\phi \int_\Omega \phi^m_h \nabla\cdot(s(\nabla\phi^{m-1}_h, \Theta^{m-1}_h)\underline{\mathbf{p}}^m_{h,1})\, dx +$$
$$\frac{1}{2}\,\|\,\tau_m M_\phi(\nabla\cdot(s(\nabla\phi^{m-1}_h, \Theta^{m-1}_h)\underline{\mathbf{p}}^m_{h,1}) - \Pi^{(0)}_h(\nabla\cdot(s(\nabla\phi^{m-1}_h, \Theta^{m-1}_h)\underline{\mathbf{p}}^m_{h,1}))) +$$
$$\Pi^{(0)}_h(\phi^m_h) - \phi^m_h + \phi^{m-1}_h - \Pi^{(0)}_h(\phi^{m-1}_h) - \tau_m M_\phi \Pi^{(0)}_h f^m_{h,1}\,\|^2_{L^2(\Omega)}.$$

Using (6.7) in (6.5) it follows that

$$\|\phi^m - \phi^m_h\|^2_{W^{1,2}(\Omega)} \lesssim (\eta^{(1)}_h)^2, \tag{6.8a}$$

where the equilibrated a posteriori error estimator $\eta^{(1)}_h$ is given by

$$(\eta^{(1)}_h)^2 := \sum_{K\in\mathcal{T}_h} (\eta^{(1)}_K)^2, \tag{6.8b}$$

$$(\eta_K^{(1)})^2 := \frac{1}{2}\tau_m M_\phi \int_K s(\nabla\phi_h^{m-1}, \Theta_h^{m-1})^2 |\nabla\phi_h^m|^2 \, dx + \int_K |\underline{\mathbf{p}}_{h,1}^m|^2 \, dx\Big) - \tag{6.8c}$$
$$\tau_m M_\phi \int_K s(\nabla\phi_h^{m-1}, \Theta_h^{m-1})\underline{\mathbf{p}}_{h,1}^m \cdot \nabla\phi_h^m \, dx + \frac{1}{2} \parallel \tau_m M_\phi(\nabla\cdot(s(\nabla\phi_h^{m-1}, \Theta_h^{m-1})\underline{\mathbf{p}}_{h,1}^m) -$$
$$\Pi_h^{(0)}(\nabla\cdot(s(\nabla\phi_h^{m-1}, \Theta_h^{m-1})\underline{\mathbf{p}}_{h,1}^m))) + \Pi_h^{(0)}(\phi_h^m) - \phi_h^m + \phi_h^{m-1} - \Pi_h^{(0)}(\phi_h^{m-1}) -$$
$$\tau_m M_\phi \Pi_h^{(0)} f_h^m \parallel_{L^2(K)}^2 .$$

6.2. A posteriori error estimator for the Θ-equation

The situation is more complicated for the Θ-equation. If we choose $V = W^{1,1}_{\Theta_D,\Gamma}(\Omega)$ and $J_P = J_P^{(2)}$, it has been shown in [22] that

$$J_D^{(2)}(\underline{\mathbf{q}}) = \frac{1}{2}\parallel \frac{\tau_m M_\Theta H}{2\xi_0}\nabla\cdot\underline{\mathbf{q}} + \Theta_h^{m-1} + \tau_m M_\Theta f_{h,2}^m\parallel_{L^2(\Omega)}^2 - \tag{6.9}$$
$$\frac{1}{2}\|\phi_h^{m-1}\|_{L^2(\Omega)}^2 + I_K(\underline{\mathbf{q}}),\ \ \underline{\mathbf{q}} \in Q = \underline{\mathbf{H}}(\mathrm{div};\Omega),$$

is the predual of $J_P^{(2)}$, i.e., $J_P^{(2)}$ is the dual of $J_D^{(2)}$, and

$$\|\Theta^m - \Theta_h^m\|_{L^2(\Omega)}^2 \lesssim J_P^{(2)}(v^m) + J_D^{(2)}(\underline{\mathbf{q}}^m) \tag{6.10}$$

for some approximation v^m of Θ^m and some $\underline{\mathbf{q}}^m \in \underline{\mathbf{H}}(\mathrm{div};\Omega)$. In (6.9) I_K stands for the indicator function of the closed convex set

$$K := \{\underline{\mathbf{q}} \in \underline{\mathbf{H}}(\mathrm{div};\Omega) \mid |\underline{\mathbf{q}}| \le 1 \text{ a.e. in } \Omega\}. \tag{6.11}$$

Natural candidates for v^m and $\underline{\mathbf{q}}^m$ are the IPDG approximation Θ_h^m and the flux function $\underline{\mathbf{p}}_{h,2}^m$ from the two-field formulation (5.22) with the numerical flux $\hat{\underline{\mathbf{p}}}_{\partial K}^m$ given by (5.23). However, $\Theta_h^m \notin W^{1,1}(\Omega)$ and $\underline{\mathbf{p}}_{h,2}^m \notin \underline{\mathbf{H}}(\mathrm{div};\Omega)$. Since $J_{h,P}^{(2)}$ is the natural extension of $J_P^{(2)}$ to $W^{1,1}(\Omega;\mathcal{T}_h)$, i.e., $J_{h,P}^{(2)}(\Theta) = J_P^{(2)}(\Theta)$ for $\Theta \in W^{1,1}(\Omega)$, we may use $J_{h,P}^{(2)}(\Theta_h^m)$ in (6.13). On the other hand, we define an equilibrated flux function $\underline{\mathbf{p}}_{h,2}^{m,eq} \in \mathrm{RT}_0(\Omega;\mathcal{T}_h)$ by specifying the degrees of freedom on each $K \in \mathcal{T}_h$ according to

$$\int_E \mathbf{n}_E \cdot \underline{\mathbf{p}}_{h,2}^{m,eq} p_0 \, ds = \int_E \mathbf{n}_E \cdot \hat{\underline{\mathbf{p}}}_{\partial K}|_E \, p_0 \, ds,\ \ p_0 \in P_0(E),\ \ E \in \mathcal{E}_h(\partial K). \tag{6.12}$$

Then, following subsection 4.1 from [22] we have

$$\|\Theta^m - \Theta_h^m\|_{L^2(\Omega)}^2 \lesssim J_{h,P}^{(2)}(\Theta_h^m) + J_D^{(2)}(\underline{\mathbf{p}}_{h,2}^{m,eq}). \tag{6.13}$$

Theorem 6.1. *The flux function $\underline{\mathbf{p}}_{h,2}^{m,eq} \in RT_0(\Omega;\mathcal{T}_h)$ is equilibrated in the sense that it satisfies*

$$\Theta_h^{(0)}(\phi_h^m) - \frac{\tau_m M_\Theta H}{2\xi_0}\nabla\underline{\mathbf{p}}_{h,2}^{m,eq} = \Pi_h^{(0)}(\Theta_h^{m-1}) + \tau_m M_\Theta \Pi_h^{(0)}(f_{h,2}^m) \text{ in each } K \in \mathcal{T}_h. \tag{6.14}$$

Proof. By Gauss' theorem and using (6.12) as well as (5.22b) with $v_h|_K = p_0 \in P_0(K)$, $v_h|_{K'} = 0, K' \neq K$, we find

$$\frac{\tau_m M_\Theta H}{2\xi_0}\int_K \nabla\cdot\underline{\mathbf{p}}_{h,2}^{m,eq} p_0 \, dx = \frac{\tau_m M_\Theta H}{2\xi_0}\int_{\partial K}\mathbf{n}_{\partial K}\cdot\underline{\mathbf{p}}_{h,2}^{m,eq} p_0 \, ds \ =$$
$$\frac{\tau_m M_\Theta H}{2\xi_0}\int_{\partial K}\mathbf{n}_{\partial K}\cdot\hat{\underline{\mathbf{p}}}_{\partial K}^m p_0 \, ds = -\int_K \Theta_h^m p_0 \, dx + \int_K \Theta_h^{m-1} p_0 \, dx +$$
$$\tau_m M_\Theta \int_K f_{h,2}^m p_0 \, dx,$$

from which we deduce that (6.14) holds true.

For practical purposes, we further replace $I_K(\underline{\mathbf{p}}_{h,2}^{m,eq})$ by the penalty term

$$\alpha_2 \sum_{K\in\mathcal{T}_h}\int_K (|\underline{\mathbf{p}}_{h,2}^{m,eq}| - 1)_+ \, dx \tag{6.15}$$

with a penalty parameter $\alpha_2 \gg 1$. Moreover, as in Section 5 we have

$$\frac{1}{2}\|\Theta_h^m - \Theta_h^{m-1}\|^2_{L^2(\Omega)} + \frac{1}{2}\sum_{K\in\mathcal{T}_h} \|\frac{\tau_m M_\Theta H}{2\xi_0}\nabla\cdot \underline{\mathbf{p}}_{h,2}^{m,eq} + \Theta_h^{m-1} + \tau_m M_\Theta f_{h,2}^m\|^2_{L^2(K)} - \tag{6.16}$$

$$\frac{1}{2}\|\Theta_h^{m-1}\|^2_{L^2(\Omega)} - \tau_m M_\Theta \sum_{K\in\mathcal{T}_h}\int_K f_{h,1}^m \Theta_h^m\, dx = \frac{\tau_m M_\Theta H}{2\xi_0}\sum_{K\in\mathcal{T}_h}\int_K \Theta_h^m \nabla\cdot \underline{\mathbf{p}}_{h,2}^{m,eq}\, dx +$$

$$\frac{1}{2}\|\Pi_h^{(0)}(\Theta_h^m) - \Theta_h^m + \Theta_h^{m-1} - \Pi_h^{(0)}(\Theta_h^{m-1}) - \tau_m M_\Theta \Pi_h^{(0)} f_{h,2}^m\|^2_{L^2(\Omega)}.$$

Using (6.15) and (6.16) in (6.13) we obtain

$$\|\Theta^m - \Theta_h^m\|^2_{L^2(\Omega)} \lesssim (\eta_h^{(2)})^2, \tag{6.17a}$$

where the equilibrated a posteriori error estimator $\eta_h^{(2)}$ is given by

$$(\eta_h^{(2)})^2 := \sum_{K\in\mathcal{T}_h}(\eta_K^{(2)})^2, \tag{6.17b}$$

$$(\eta_K^{(2)})^2 := \frac{\tau_m M_\Theta H}{2\xi_0}\int_K f_{ori}(\omega(\phi_h^m), \nabla_{DG}\Theta_h^m)\, dx + \frac{\alpha_1}{2}\sum_{E\in\partial K\setminus(K\cap\Gamma)} |[\Theta_h^m]_E|\, ds\ + \tag{6.17c}$$

$$\tau_m M_\Theta \int_K \Theta_h^m \nabla\cdot \underline{\mathbf{p}}_{h,2}^{m,eq}\, dx + \frac{1}{2}\ \|\ \Pi_h^{(0)}(\Theta_h^m) - \Theta_h^m + \Theta_h^{m-1} - \Pi_h^{(0)}(\Theta_h^{m-1}) -$$

$$\tau_m M_\Theta \Pi_h^{(0)} f_{h,2}^m\ \|^2_{L^2(K)} + \alpha_2 \int_K (|\underline{\mathbf{p}}_{h,2}^{m,eq}| - 1)_+\, dx.$$

The realization of the adaptivity in space is done by Dörfler marking [23] with bulk parameter $0 < \kappa < 1$ and longest edge bisection. At each time step, we start from an initial coarse triangulation $\mathcal{T}_{h_0}$ and apply the equilibrated a posteriori error estimator $\eta_h^{(1)}$ first resulting in a final triangulation $\mathcal{T}_{h_f}$. This triangulation $\mathcal{T}_{h_f}$ is then used as an initial mesh for the adaptivity in Θ based on the equilibrated a posteriori error estimator $\eta_h^{(2)}$. The reason for this strategy is that there are local regions of steep gradients for both ϕ and Θ at the interfaces between areas of full and zero crystallinity, whereas for Θ there are additional regions of steep gradients within the areas of full crystallinity due to changes in the orientation angle.

7. Adaptive time stepping

The time adaptivity used in this paper is dictated by the convergence of a semismooth Newton method for the numerical solution of the nonlinear IPDG approximation (5.18) and not by an upper bound for the discretization error in time, because the time steps predicted by the latter are much larger than those by the former.

Setting $\mathbf{\Theta}^m := (\Theta_1^m, \ldots, \Theta_{N_h}^m)^T$, $N_h := \dim V^2_{h,0,\Gamma}$, the algebraic formulation of (5.18) leads to a nonlinear system of the form

$$\mathbf{F}(\mathbf{\Theta}^m, t_m) = \mathbf{0}, \tag{7.1}$$

with a nonlinear mapping $\mathbf{F} : \mathbb{R}^{N_h}\times\mathbb{R}_+ \to \mathbb{R}^{N_h}$ that is not differentiable in $\mathbf{\Theta}^m$ in the classical sense, but admits a generalized Jacobian $\partial_{\mathbf{\Theta}}\mathbf{F}$ in the sense of Clarke [24]. Hence, the nonlinear system (7.1) can be solved by a semismooth Newton method (cf., e.g., [25]). The problem is the appropriate choice of the time step sizes τ_m, $1 \le m \le M$, in order to guarantee convergence. In fact, a uniform choice $\tau_m = T/M$ only works, if M is chosen sufficiently large which would require an unnecessary huge amount of time steps. An appropriate way to overcome this difficulty is to consider (7.1) as a parameter dependent nonlinear system with the time as a parameter and to apply a predictor–corrector continuation strategy with an adaptive choice of the time steps (cf., e.g., [3,5,26,27]). Given $\mathbf{\Theta}^{m-1}$, the time step size $\tau_{m-1,0} = \tau_{m-1}$, and setting $k = 0$, where k is a counter for the predictor–corrector steps, the predictor step for (7.1) consists of constant continuation leading to the initial guesses

$$\mathbf{\Theta}^{(m,k)} = \mathbf{\Theta}^{m-1}, \quad t_m = t_{m-1} + \tau_{m-1,k}. \tag{7.2}$$

Setting $\nu_1 = 0$ and $\mathbf{\Theta}^{(m,k,\nu_1)} = \mathbf{\Theta}^{(m,k)}$, for $\nu_1 \le \nu_{max}$, where $\nu_{max} > 0$ is a pre-specified maximal number, the semismooth Newton iteration

$$\partial_{\mathbf{\Theta}}\mathbf{F}(\mathbf{\Theta}^{(m,k,\nu_1)}, \mathbf{\Phi}^{m-1}, t_m)\mathbf{\Delta\Theta}^{(m,k,\nu_1)} \ni -\mathbf{F}(\mathbf{\Theta}^{(m,k,\nu_1)}, \mathbf{\Phi}^{m-1}, t_m), \tag{7.3}$$

$$\mathbf{\Theta}^{(m,k,\nu_1+1)} = \mathbf{\Theta}^{(m,k,\nu_1)} + \mathbf{\Delta\Theta}^{(m,k,\nu_1)}, \quad \nu_1 \ge 0,$$

Table 1
Physical data: Mobilities M_Θ, M_ϕ, parameter ε_r in the interpolation function ω, modulus of anisotropy s_0, symmetry index m_s.

M_ϕ	M_Θ	ε_r	s_0		m_s	
			Ex. 1	Ex. 2	Ex. 1	Ex. 2
$1.5 \cdot 10^2$	$1.1 \cdot 10^1$	$1.0 \cdot 10^{-3}$	0.0	0.2	–	2

serves as a corrector whose convergence is monitored by the contraction factor

$$\Lambda_\Theta^{(m,k,\nu_1)} = \frac{\|\overline{\boldsymbol{\Delta\Theta}^{(m,k,\nu_1)}}\|}{\|\boldsymbol{\Delta\Theta}^{(m,k,\nu_1)}\|}, \tag{7.4}$$

where $\overline{\boldsymbol{\Delta\Theta}^{(m,k,\nu_1)}}$ is the solution of the auxiliary Newton step

$$\partial_{\boldsymbol{\Theta}}\mathbf{F}(\boldsymbol{\Theta}^{(m,k,\nu_1)}, \boldsymbol{\Phi}^{m-1}, t_m)\overline{\boldsymbol{\Delta\Theta}^{(m,k,\nu_1)}} \ni -\mathbf{F}(\boldsymbol{\Theta}^{(m,k,\nu_1+1)}, \boldsymbol{\Phi}^{m-1}, t_m). \tag{7.5}$$

If the contraction factor satisfies

$$\Lambda_\Theta^{(m,k,\nu_1)} < \frac{1}{2}, \tag{7.6}$$

we set $\nu_1 = \nu_1 + 1$. If $\nu_1 > \nu_{max}$, both the Newton iteration and the predictor–corrector continuation strategy are terminated indicating non-convergence. Otherwise, we continue the semismooth Newton iteration (7.3). If (7.6) does not hold true, we set $k = k + 1$ and the time step is reduced according to

$$\tau_{m,k} = \max\left(\frac{\sqrt{2}-1}{\sqrt{4\Lambda_\Theta^{(m,k,\nu_1)}+1}-1}\,\tau_{m,k-1}, \tau_{min}\right), \tag{7.7}$$

where $\tau_{min} > 0$ is some pre-specified minimal time step. If $\tau_{m,k} > \tau_{min}$, we go back to the prediction step (7.2). Otherwise, the predictor–corrector strategy is stopped indicating non-convergence. The semismooth Newton iteration is terminated successfully, if for some $\nu_1^* > 0$ the relative error of two subsequent semismooth Newton iterates satisfies

$$\frac{\|\boldsymbol{\Theta}^{(m,k,\nu_1^*)} - \boldsymbol{\Theta}^{(m,k,\nu_1^*-1)}\|}{\|\boldsymbol{\Theta}^{(m,k,\nu_1^*)}\|} < \varepsilon_T \tag{7.8}$$

for some pre-specified accuracy $\varepsilon_T > 0$.

In this case, we set

$$\boldsymbol{\Theta}^m = \boldsymbol{\Theta}^{(m,k,\nu_1^*)} \tag{7.9}$$

and predict a new time step according to

$$\tau_m = \frac{(\sqrt{2}-1)\,\|\boldsymbol{\Delta\Theta}^{(m,k,0)}\|}{2\Lambda_\Theta^{(m,k,0)}\,\|\boldsymbol{\Theta}^{(m,k,0)} - \boldsymbol{\Theta}^m\|}\,\tau_{m,k}, \tag{7.10}$$

where amp > 1 is a pre-specified amplification factor for the time step sizes. We set $m = m + 1$ and begin new predictor–corrector iterations for the time interval $[t_m, t_{m+1}]$.

In principle, we could include the same strategy for the ϕ-iterates as has been done in [3,5]. However, as it turned out, once the time-step τ_m is accepted for the Θ-iterate, it is also accepted for the ϕ-iterate. Therefore, we decided to restrict ourselves to the predictor–corrector continuation strategy for the Θ-iterates.

8. Numerical results

We have applied the space–time adaptive splitting method to two illustrative examples. The first example is about the growth of four crystals of different orientation angles initially located at the four corners of the computational domain (cf. Fig. 3), whereas the second example deals with the spherulitic growth of a single crystal initially located at the center of the computational domain (cf. Fig. 5). The physical data we have used are depicted in Tables 1 and 2. In particular, in Example 2 the constants r_1 and r_2 for the orientational free energy density are chosen such that the angle of misorientation is 30^o leading to six preferred orientations. The computational domain is $\Omega = (0\mu m, 6\mu m)^2$. Table 3 contains the computational data for the spatial discretization and the predictor–corrector continuation strategy.

Example 1. We consider the isotropic growth (i.e., $s_0 = 0$) of four single crystals with different orientation angles. The initial orientation angles Θ_0, the initial local degree of crystallinity ϕ_0, and the boundary data ϕ_D are given as follows (cf. Fig. 3):

$$\phi_0 = \begin{array}{l} 1.0 \text{ (red) around the four corners,} \\ 0.0 \text{ (white) elsewhere.} \end{array}$$

Table 2
Physical data: Free energy H of low grain boundaries, correlation length ξ_0 of the orientational field, constants r_1, r_2, δ determining the orientational free energy density f_{ori}.

H	ξ_0	r_1		r_2		δ	
		Ex. 1	Ex. 2	Ex. 1	Ex. 2	Ex. 1	Ex. 2
$1.0 \cdot 10^{-3}$	$2.1 \cdot 10^{-4}$	–	3.0	–	0.5	–	0.2

Table 3
Computational data for the spatial discretization and the predictor–corrector continuation strategy: regularization parameter λ for the Moreau–Yosida approximation of the subdifferential of the orientational free energy density, mesh width h for the initial triangulation of the computational domain, maximum number ν_{max} of semismooth Newton iterations, minimum time step size τ_{min}, relative accuracy ε_T of semismooth Newton iterations, and amplification factor amp for new time step size.

λ	h		ν_{max}	τ_{min}	ε_T	amp
	Ex. 1	Ex. 2				
$1.0 \cdot 10^{-3}$	0.75 μm	1.5 μm	50	$1.0 \cdot 10^{-6}$	$1.0 \cdot 10^{-3}$	1.2

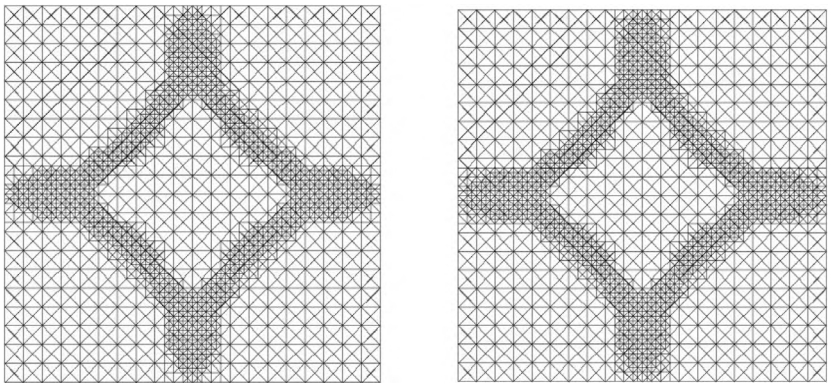

Fig. 2. Example 1: Adaptively generated meshes at time $t = 2.3 \cdot 10^{-4}$ s. Left: Local degree of crystallinity. Right: Orientation angle.

$$\Theta_0 = \begin{cases} 1.2\pi \text{ (red) around the right upper corner,} \\ 1.0\pi \text{ (yellow) around the right lower corner,} \\ 0.8\pi \text{ (blue) around the left lower corner,} \\ 0.6\pi \text{ (green) around the left upper corner,} \\ 0.9 \pm 0.05\pi \text{ randomly chosen elsewhere.} \end{cases}$$

The boundary data are $\phi_D = \phi_0|_\Gamma$, $\Theta_D = \Theta_0|_\Gamma$.

The four crystals grow along the curvature and start to impinge on each other with the star-shaped area of local degree of crystallinity $\phi = 0$ shrinking (cf. Figs. 3 and Fig. 4). For better visibility we have suppressed the values of Θ as well as the refinements with respect to Θ in the areas of zero crystallinity.

Fig. 2 displays the adaptively generated meshes for the local degree of crystallinity ϕ (left) and for the angle of orientation Θ (right) and Fig. 3 shows the local degree of crystallinity ϕ (left) and the angle of orientation Θ (right) at time $t = 2.3 \cdot 10^{-4}$ shortly after the onset of the isotropic growth of the four crystals. We observe significant refinements around the interfaces between the area of full crystallinity ($\phi = 1$) and the area of zero crystallinity ($\phi = 0$). Since at that time the impingement of the four crystals is small, the adaptively generated mesh for the angle of orientation Θ is almost the same as the mesh for the local degree of crystallinity ϕ.

Likewise, in Fig. 4 the adaptively generated meshes are shown for the local degree of crystallinity ϕ (left) and for the angle of orientation Θ (right) at the advanced time $t = 7.5 \cdot 10^{-3}$, whereas Fig. 5 displays the local degree of crystallinity ϕ (left) and the angle of orientation Θ (right) at that time. We see that the four crystals have substantially grown in radial direction. As far as the adaptive refinement in space is concerned, for ϕ there are only refinements around the interfaces between the area of full crystallinity ($\phi = 1$) and the area of zero crystallinity ($\phi = 0$) (Fig. 4 (left)), whereas for Θ we have additional refinements at the interfaces between regions of different orientation angles (Fig. 4 (right)).

Example 2. We consider the formation of a Category 1 spherulite from a nucleation site which is initially occupying a subdomain Ω_0 around the center of the computational domain Ω. The initial data are given by $\phi_0 = 1.0$ in Ω_0 and

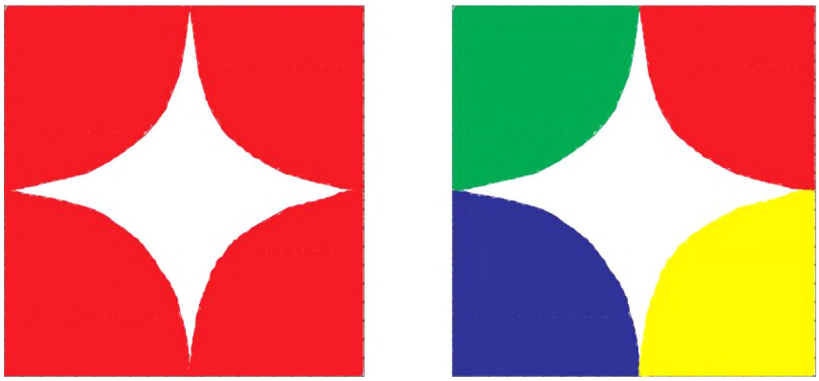

Fig. 3. Example 1: Local degree of crystallinity (left) and orientation angle (right) at time $t = 2.3 \cdot 10^{-4}$.

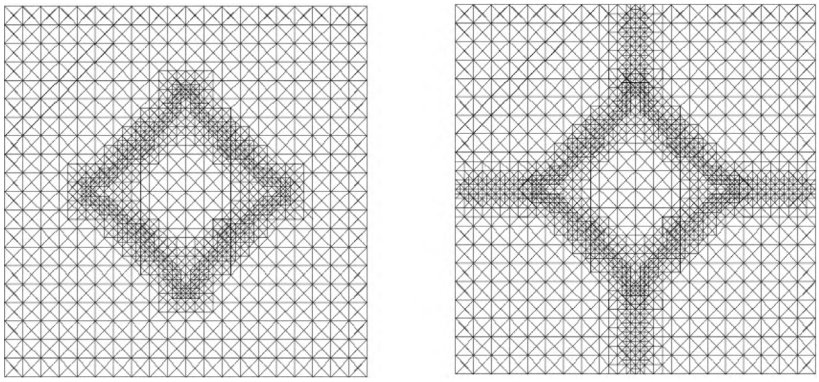

Fig. 4. Example 1: Adaptively generated meshes at time $t = 7.5 \cdot 10^{-3}$ *s*. Left: Local degree of crystallinity. Right: Orientation angle.

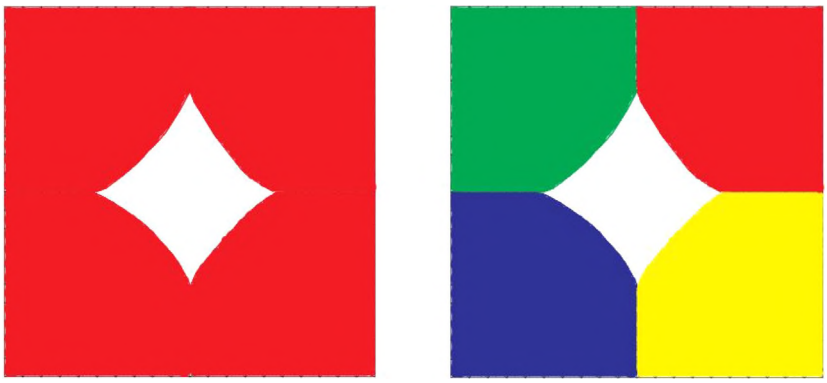

Fig. 5. Example 1: Local degree of crystallinity (left) and orientation angle (right) at time $t = 7.5 \cdot 10^{-3}$.

$\phi = 0.0$ elsewhere and by Θ_0 varying between 0.7π and 1.2π in Ω_0 and chosen randomly around 0.95π elsewhere. In particular, the assignment of the colors in Figs. 7 and 9 is as follows: Blue (1.2π), Brown (1.0π), Cyan (0.9π), Green (0.8π), Red (1.1π), and Yellow (0.7π). The boundary data are $\phi_D = \Theta_D = 0$.

Again, for better visibility we have suppressed the values of Θ as well as the refinements with respect to Θ in the areas of zero crystallinity.

Fig. 6 displays the adaptively generated meshes for the local degree of crystallinity ϕ (left) and for the angle of orientation Θ (right) at time $t = 1.1 \cdot 10^{-4}$ shortly after the beginning of the spherulitic growth. Due to the initial smallness of the crystal, the two meshes do not differ significantly. The associated Fig. 7 shows the local degree of crystallinity ϕ (left) and the angle of orientation Θ (right) at that time. Likewise, Fig. 8 contains the adaptively generated meshes for the local degree of crystallinity ϕ (left) and for the angle of orientation Θ (right) at time $t = 4.7 \cdot 10^{-3}$ when crystalline

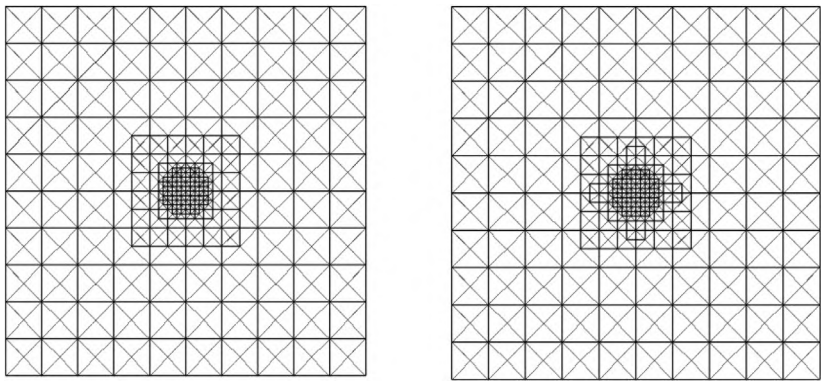

Fig. 6. Example 2: Adaptively generated meshes at time $t = 1.1 \cdot 10^{-4}$ *s*. Left: Local degree of crystallinity. Right: Orientation angle.

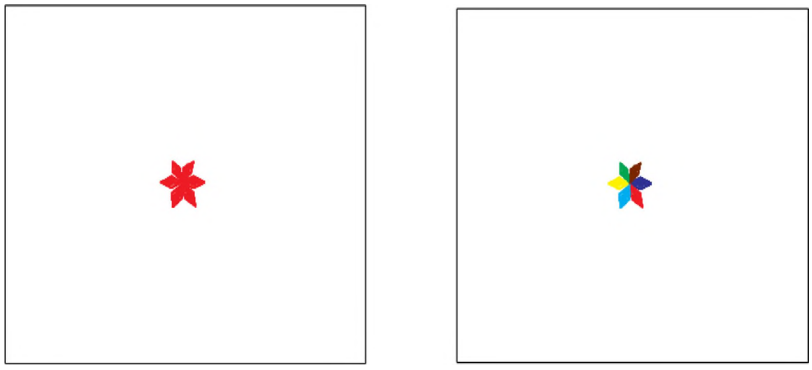

Fig. 7. Example 2: Local degree of crystallinity (left) and orientation angle (right) at time $t = 1.1 \cdot 10^{-4}$.

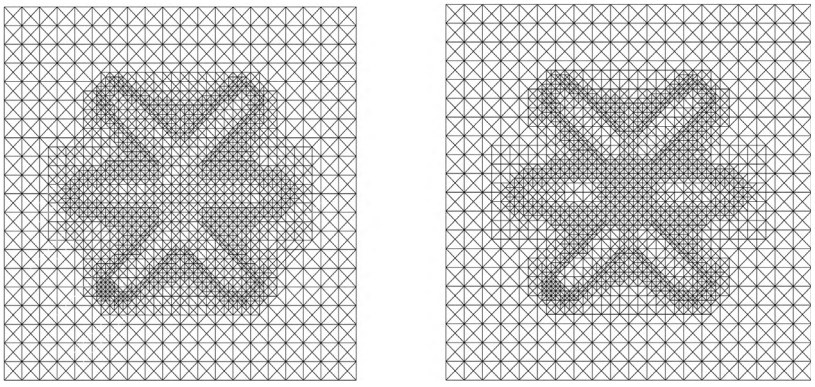

Fig. 8. Example 2: Adaptively generated meshes at time $t = 4.7 \cdot 10^{-3}$ *s*. Left: Local degree of crystallinity. Right: Orientation angle.

branching has already set in. As in Example 1, there is a pronounced refinement of the mesh for the local degree of crystallinity at the interface between the area of full crystallinity ($\phi = 1$) and the area of zero crystallinity ($\phi = 0$) where steep gradients occur. On the other hand, there is additional refinement of the mesh for the angle of orientation at the interfaces between areas of different orientation angles which are located around the center of the computational domain. Fig. 9 displays the local degree of crystallinity ϕ (left) and the angle of orientation Θ (right) at that time.

Finally, Figs. 10 and 11 show the history of the predictor–corrector strategy where the adaptively chosen time steps are shown as a function of the number of iterations for Example 1 and Example 2. We observe large fluctuations in the time steps which are due the occurrence of very steep gradients at the growing front, particularly when crystalline branching takes place.

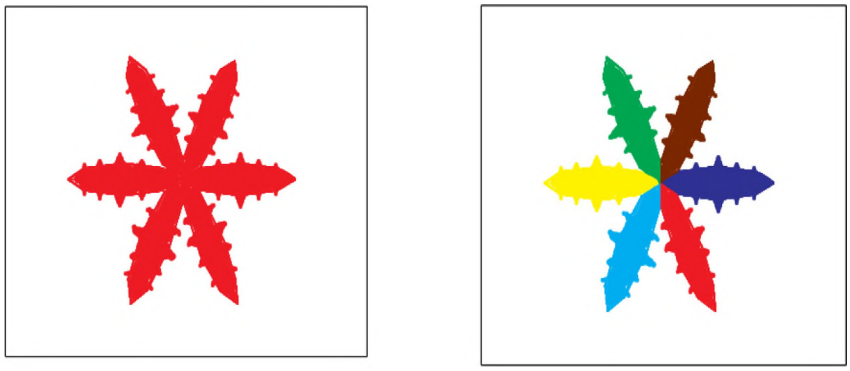

Fig. 9. Example 2: Local degree of crystallinity (left) and orientation angle (right) at time $t = 4.7 \cdot 10^{-3}$.

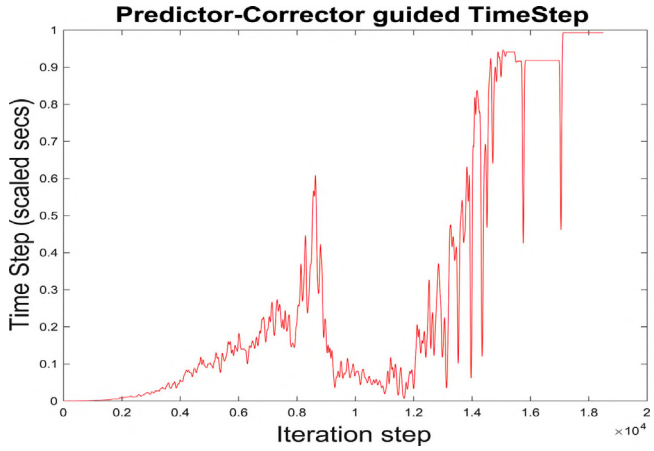

Fig. 10. Performance of the predictor–corrector continuation strategy. Adaptive choice of time steps τ_m: Example 1.

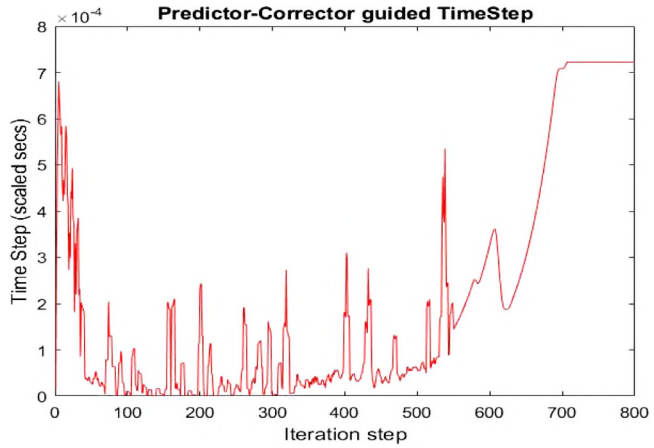

Fig. 11. Performance of the predictor–corrector continuation strategy. Adaptive choice of time steps τ_m: Example 2 (right).

References

[1] L. Gránásy, T. Pusztai, J.A. Warren, Modeling polycrystalline solidification using phase field theory, J. Phys. Condens. Matter. 16 (2004)

R1205–R1235.
[2] L. Gránásy, L. Ratkai, A. Szallas, B. Korbuly, G. Toth, L. Környei, T. Pusztai, Phase-field modeling of polycrystalline solidification: from needle crystals to spherulites ; a review, Metall. Mater. Trans. A 45A (2014).
[3] R.H.W. Hoppe, J.J. Winkle, A splitting scheme for the numerical solution of the Kobayashi-Warren-Carter system, Numer. Math. Theory Methods Appl. 12 (2019) 661–680.
[4] R.H.W. Hoppe, B. Pahari, J.J. Winkle, Numerical simulation of the formation of spherulites in polycrystalline binary mixtures, Appl. Numer. Math. 166 (2021) 61–75.
[5] R.H.W. Hoppe, J.J. Winkle, Numerical solution of a phase field model for polycrystallization processes in binary mixtures, Comput. Vis. Sci. 20 (2019) 13–27.
[6] D. Braess, T. Fraunholz, R.H.W. Hoppe, An equilibrated a posteriori error estimator for the interior penalty discontinuous Galerkin method, SIAM J. Numer. Anal. 52 (2014) 2121–2136.
[7] Z. Cai, S. Zhang, Flux recovery and a posteriori error estimators: Conforming elements for scalar elliptic equations, SIAM J. Numer. Anal. 48 (2010) 578–602.
[8] Z. Cai, S. Zhang, Robust equilibrated residual error estimator for diffusion problems: conforming elements, SIAM J. Numer. Anal. 50 (2012) 151–170.
[9] S. Cochez-Dhondt, S. Nicaise, Equilibrated error estimators for discontinuous Galerkin methods, Numer. Methods Partial Differential Equations 24 (2008) 1236–1252.
[10] A. Ern, S. Nicaise, M. Vohralík, An accurate H(div) flux reconstruction for discontinuous Galerkin approximations of elliptic problems, C. R. Acad. Sci., Paris I 345 (2007) 709–712.
[11] A. Ern, M. Vohralík, Flux reconstruction and a posteriori error estimation for discontinuous Galerkin methods on general nonmatching grids, C. R. Acad. Sci., Paris I 347 (2009) 4441–4444.
[12] R. Kobayashi, J.A. Warren, W.C. Carter, A continuum model of grain boundaries, Physica D 140 (2000) 141–150.
[13] L.C. Evans, Weak Convergence Methods for Nonlinear Partial Differential Equations, in: CBMS Regional Conference Series in Mathematics, vol. 74, American Mathematical Society, Providence, 1990.
[14] H. Attouch, G. Buttazzo, G. Michaille, Variational Analysis in Sobolev and BV Spaces, in: The MPS/SIAM Series on Optimization, vol. 6, SIAM, Philadelphia, 2006.
[15] L. Ambrosio, N. Fusco, D. Pallara, Functions of Bounded Variation and Free Discontinuity Problems, Oxford University Press, New York, 2000.
[16] L. Gránásy, T. Pusztai, G. Tegze, J.A. Warren, J.F. Douglas, Growth and form of sperulites, Phys. Rev. E 011605 (2005).
[17] I. Ekeland, R. Temam, Convex Analysis and Variational Problems, SIAM, Philadelphia, 1999.
[18] P.G. Ciarlet, The Finite Element Method for Elliptic Problems, SIAM, Philadelphia, 2002.
[19] A. Buffa, C. Ortner, Compact embeddings of broken Sobolev spaces and applications, IMA J. Numer. Anal. 29 (2009) 827–855.
[20] L. Diening, D. Kröner, M. Ruzicka, I. Toulopoulos, A local discontinuous Galerkin approximation for systems with p-structure, IMA J. Numer. Anal. 34 (2013) 1447–1488.
[21] S.I. Repin, A posteriori error estimation for variational problems with uniformly convex functionals, Math. Comp. 69 (2000) 481—500.
[22] S. Bartels, Error control and adaptivity for a variational model problem defined on functions of bounded variation, Math. Comp. 84 (2015) 1217–1240.
[23] W. Dörfler, A convergent adaptive algorithm for Poisson's equation, SIAM J. Numer. Anal. 33 (1996) 1106–1124.
[24] F.H. Clarke, Optimization and Nonsmooth Analysis, Wiley, New York, 1983.
[25] M. Hintermüller, Semismooth Newton methods and applications, in: Notes of the Oberwolfach-Seminar on 'Mathematics of PDE-Constrained Optimization', Math. Research Institute at Oberwolfach, Oberwolfach, 2010.
[26] P. Deuflhard, Newton Methods for Nonlinear Problems - Affine Invariance and Adaptive Algorithms, Springer, Berlin, Heidelberg, New York, 2004.
[27] R.H.W. Hoppe, C. Linsenmann, An adaptive Newton continuation strategy for the fully implicit finite element immersed boundary method, J. Comput. Phys. 231 (2012) 4676–4693.